





## Article

# GABA<sub>A</sub> and GABA<sub>B</sub> Receptors Mediate GABA-Induced Intracellular Ca<sup>2+</sup> Signals in Human Brain Microvascular Endothelial Cells

Sharon Negri <sup>1</sup>, Francesca Scolari <sup>2</sup>, Mauro Vismara <sup>3</sup>, Valentina Brunetti <sup>1</sup>, Pawan Faris <sup>1</sup>, Giulia Terribile <sup>4,5</sup>, Giulio Sancini <sup>4,5</sup>, Roberto Berra-Romani <sup>6</sup> and Francesco Moccia <sup>1,\*</sup>

- <sup>1</sup> Laboratory of General Physiology, Department of Biology and Biotechnology “L. Spallanzani”, University of Pavia, 27100 Pavia, Italy
- <sup>2</sup> Institute of Molecular Genetics (IGM)-CNR “Luigi Luca Cavalli-Sforza”, 27100 Pavia, Italy
- <sup>3</sup> Laboratory of Biochemistry, Department of Biology and Biotechnology “L. Spallanzani”, University of Pavia, 27100 Pavia, Italy
- <sup>4</sup> School of Medicine and Surgery, University of Milano-Bicocca, 20900 Monza, Italy
- <sup>5</sup> Nanomedicine Center, Neuroscience Center, School of Medicine and Surgery, University of Milano-Bicocca, 20900 Monza, Italy
- <sup>6</sup> Department of Biomedicine, School of Medicine, Benemérita Universidad Autónoma de Puebla, Puebla 74325, Mexico
- \* Correspondence: francesco.moccia@unipv.it; Tel.: +39-0382-987613



**Citation:** Negri, S.; Scolari, F.; Vismara, M.; Brunetti, V.; Faris, P.; Terribile, G.; Sancini, G.; Berra-Romani, R.; Moccia, F. GABA<sub>A</sub> and GABA<sub>B</sub> Receptors Mediate GABA-Induced Intracellular Ca<sup>2+</sup> Signals in Human Brain Microvascular Endothelial Cells. *Cells* **2022**, *11*, 3860. <https://doi.org/10.3390/cells11233860>

Academic Editor: María Teresa Alonso

Received: 20 October 2022

Accepted: 28 November 2022

Published: 30 November 2022

**Publisher’s Note:** MDPI stays neutral with regard to jurisdictional claims in published maps and institutional affiliations.



**Copyright:** © 2022 by the authors. Licensee MDPI, Basel, Switzerland. This article is an open access article distributed under the terms and conditions of the Creative Commons Attribution (CC BY) license (<https://creativecommons.org/licenses/by/4.0/>).

**Abstract:** Numerous studies recently showed that the inhibitory neurotransmitter,  $\gamma$ -aminobutyric acid (GABA), can stimulate cerebral angiogenesis and promote neurovascular coupling by activating the ionotropic GABA<sub>A</sub> receptors on cerebrovascular endothelial cells, whereas the endothelial role of the metabotropic GABA<sub>B</sub> receptors is still unknown. Preliminary evidence showed that GABA<sub>A</sub> receptor stimulation can induce an increase in endothelial Ca<sup>2+</sup> levels, but the underlying signaling pathway remains to be fully unraveled. In the present investigation, we found that GABA evoked a biphasic elevation in [Ca<sup>2+</sup>]<sub>i</sub> that was initiated by inositol-1,4,5-trisphosphate- and nicotinic acid adenine dinucleotide phosphate-dependent Ca<sup>2+</sup> release from neutral and acidic Ca<sup>2+</sup> stores, respectively, and sustained by store-operated Ca<sup>2+</sup> entry. GABA<sub>A</sub> and GABA<sub>B</sub> receptors were both required to trigger the endothelial Ca<sup>2+</sup> response. Unexpectedly, we found that the GABA<sub>A</sub> receptors signal in a flux-independent manner via the metabotropic GABA<sub>B</sub> receptors. Likewise, the full Ca<sup>2+</sup> response to GABA<sub>B</sub> receptors requires functional GABA<sub>A</sub> receptors. This study, therefore, sheds novel light on the molecular mechanisms by which GABA controls endothelial signaling at the neurovascular unit.

**Keywords:** hCMEC/D3 cells; GABA; GABA<sub>A</sub> receptors; GABA<sub>B</sub> receptors; Ca<sup>2+</sup> signaling; InsP<sub>3</sub> receptors; two-pore channels; store-operated Ca<sup>2+</sup> entry

## 1. Introduction

The neurotransmitter  $\gamma$ -aminobutyric acid (GABA) is not only crucial to maintain a proper excitatory:inhibitory balance in neuronal networks by inhibiting glutamatergic pyramidal neurons [1–3], but is also instrumental to generate synchronized network oscillations that underpin optimal cognitive functions [4,5]. GABA dampens neuronal excitability by gating Cl<sup>−</sup>-permeable GABA<sub>A</sub> receptors, thereby enabling Cl<sup>−</sup> influx down the electrochemical gradient and hyperpolarizing the membrane potential [4]. GABA<sub>A</sub> receptors typically consist of pentameric channels formed by the combination of three distinct subunits, according to the following stoichiometry: 2 $\alpha$ :2 $\beta$ :1 $\gamma$  [3,6]. GABA-dependent inhibition of neurotransmitter release and neuronal activity may also be mediated by metabotropic G<sub>i/o</sub> protein-coupled GABA<sub>B</sub> receptors, which are widely distributed in the central nervous system [7,8]. GABA<sub>B</sub> receptors are composed of an obligatory heterodimer of the GABA<sub>B1</sub> and GABA<sub>B2</sub> subunits and induce slow postsynaptic inhibitory potentials

by stimulating  $G_{i/o}$  protein-coupled inward-rectifying  $K^+$  channels (GIRK) [7,8]. In addition, it has been documented that  $GABA_B$  receptors can induce an increase in intracellular  $Ca^{2+}$  concentrations ( $[Ca^{2+}]_i$ ) in rat cortical neurons [9] and mouse cerebellar granule neurons [10].  $GABA_B$  receptors trigger intracellular  $Ca^{2+}$  signals via a signaling pathway that utilizes heterotrimeric  $G_{i/o}$  proteins to stimulate phospholipase  $C\beta$  ( $PLC\beta$ ) and cleave phosphatidylinositol 4,5-bisphosphate ( $PIP_2$ ) into the two intracellular second messengers inositol-1,4,5-trisphosphate ( $InsP_3$ ) and diacylglycerol (DAG).  $InsP_3$ , in turn, binds to  $InsP_3$  receptors ( $InsP_3Rs$ ), which are located on the endoplasmic reticulum (ER), and promotes  $Ca^{2+}$  release into the cytoplasm. The following reduction in ER  $Ca^{2+}$  levels activates a  $Ca^{2+}$  entry pathway that resides on the plasma membrane, known as store-operated  $Ca^{2+}$  entry (SOCE), which prolongs over time the  $Ca^{2+}$  response to  $GABA_B$  receptor stimulation [9–11].

$GABAergic$  signaling within the neurovascular unit (NVU) has also been described in non-neuronal cells, including astrocytes [12,13] and cerebrovascular endothelial cells [14]. Cortical microvessels, as well as perivascular astrocytes, receive an extensive  $GABAergic$  input from local  $GABA$  interneurons [15]. Moreover, it has been clearly demonstrated that, during brain development, the pre-formed vascular network guides the tangential journey of  $GABAergic$  neurons from the dorsal to the basal telencephalon [16]. Thus,  $GABAergic$  neurons can establish a bidirectional communication with cerebrovascular endothelial cells to effectively coordinate these neurovascular interactions [16,17]. Mouse brain microvascular endothelial cells are endowed with the  $\alpha 1$ ,  $\alpha 2$ ,  $\alpha 6$ ,  $\beta 1$ ,  $\beta 2$ ,  $\beta 3$ ,  $\gamma 1$ ,  $\gamma 2$  and  $\gamma 3$  subunits of  $GABA_A$  receptors [18], while only functional evidence has been documented in favor of  $GABA_B$  receptor expression [19]. The role played by endothelial  $GABA_A$  receptors at the NVU has gathered growing interest upon the discovery that they control cerebral angiogenesis [17] and guide the radial migration of  $GABA$  interneurons [16] during embryonic development in mice, and regulate cerebral blood flow (CBF) and prevent neurological deficits in the adult [20]. The signaling pathways that are activated downstream of  $GABA_A$  receptors in cerebrovascular endothelial cells are yet to be fully unraveled [21]. Preliminary evidence showed that muscimol, a selective  $GABA_A$  receptor agonist, induced an inward  $Cl^-$  current and a transient increase in  $[Ca^{2+}]_i$  in mice cerebrovascular endothelial cells [17]. Nevertheless, it is unclear how the inward (i.e., hyperpolarizing) current carried by the ionotropic  $GABA_A$  receptors could elevate the  $[Ca^{2+}]_i$  in  $GABA$ -stimulated cells. Of note, recent studies have revealed that  $GABA_A$  receptors may trigger a metabotropic (i.e., flux-independent) signaling pathway that leads to  $InsP_3$ -induced  $Ca^{2+}$  release from the ER [22–24]. Since an increase in endothelial  $[Ca^{2+}]_i$  regulates both angiogenesis [25,26] and CBF [27,28], deciphering the mechanisms whereby  $GABA$  induces intracellular  $Ca^{2+}$  signals is mandatory to understand the molecular interactions between inhibitory interneurons and adjacent microvessels.

The hCMEC/D3 cell line represents the most suitable *in vitro* model of human cerebral microvascular endothelial cells [29,30] and has been largely exploited to unveil how cerebrovascular endothelium perceives and transduces neural activity with an increase in  $[Ca^{2+}]_i$  [27,31]. For instance, acetylcholine [32], adenosine trisphosphate (ATP) [33,34], glutamate [35], and histamine [36] bind to their specific  $G_q$ -protein coupled receptors ( $G_qPCRs$ ) and stimulate  $PLC\beta$  to trigger  $InsP_3$ -dependent  $Ca^{2+}$  release from the ER. This initial  $Ca^{2+}$  peak can be supported by lysosomal  $Ca^{2+}$  mobilization through two-pore channels 1 and 2 (respectively, TPC1 and TPC2) and is maintained over time by SOCE activation [27,31]. Intriguingly, the ionotropic N-methyl-D-aspartate (NMDA) receptors (NMDARs) were recently shown to signal an increase in  $[Ca^{2+}]_i$  in hCMEC/D3 cells in a flux-independent mode by interacting with metabotropic glutamate receptors [37]. Herein, we adopted an array of approaches, ranging from real-time quantitative reverse transcription PCR (qRT-PCR) to single-cell Fura-2 imaging to investigate the mechanisms whereby  $GABA$  elicits intracellular  $Ca^{2+}$  signals in hCMEC/D3 cells. We found that both  $GABA_A$  and  $GABA_B$  receptors are expressed and that  $GABA$  triggers a biphasic increase in  $[Ca^{2+}]_i$ . Pharmacological manipulation revealed that  $GABA$ -induced intracellular  $Ca^{2+}$  release was mediated by ER  $Ca^{2+}$  mobilization through  $InsP_3Rs$  and lysosomal  $Ca^{2+}$  discharge via

TPC1-2, whereas  $\text{Ca}^{2+}$  entry was mediated by SOCE. However,  $\text{GABA}_A$  receptors did not mediate any detectable inward current, but they rather signaled in a flux-independent manner to cause intracellular  $\text{Ca}^{2+}$  release. Conversely, the selective stimulation of  $\text{GABA}_B$  receptors induced the expected metabotropic  $\text{Ca}^{2+}$  signal that has been described in other cell types. Intriguingly, we provide evidence that  $\text{GABA}_A$  and  $\text{GABA}_B$  receptors interact to elicit a full  $\text{Ca}^{2+}$  response to GABA in hCMEC/D3 cells. These data provide the first elucidation of the signaling pathways whereby GABA can increase the  $[\text{Ca}^{2+}]_i$  in cerebrovascular endothelial cells.

## 2. Materials and Methods

### 2.1. Cell Culture

Human cerebral microvascular endothelial cells (hCMEC/D3) were obtained from the Institut National de la Santé et de la Recherche Médicale (INSERM, Paris, France). hCMEC/D3 cells cultured between passage 25 and 35 were used. As described in [38], the cells were seeded at a concentration of 27,000 cells/cm<sup>2</sup> and grown in tissue culture flasks coated with 0.1 mg/mL rat tail collagen type 1, in the following medium: EBM-2 medium (Lonza, Basel, Switzerland) supplemented with 5% fetal bovine serum, 1% penicillin–streptomycin, 1.4 μM hydrocortisone, 5 μg/mL ascorbic acid, 1/100 chemically defined lipid concentrate (Life Technologies, Milan, Italy), 10 mM HEPES and 1 ng/mL basic fibroblast growth factor. The cells were cultured at 37 °C, 5% CO<sub>2</sub> saturated humidity.

### 2.2. Solutions

Physiological salt solution (PSS) had the following composition (in mM): 150 NaCl, 6 KCl, 1.5 CaCl<sub>2</sub>, 1 MgCl<sub>2</sub>, 10 glucose, 10 HEPES. In  $\text{Ca}^{2+}$ -free solution (0 $\text{Ca}^{2+}$ ),  $\text{Ca}^{2+}$  was substituted with 2 mM NaCl, and 0.5 mM EGTA was added. Solutions were titrated to pH 7.4 with NaOH. The osmolality of PSS as measured with an osmometer (Wescor 5500, Logan, UT, USA) was 300–310 mOsm/L.

### 2.3. $[\text{Ca}^{2+}]_i$ Imaging

We utilized the  $\text{Ca}^{2+}$  imaging set-up that we have described elsewhere [32]. hCMEC/D3 cells were loaded with 4 μM Fura-2 acetoxymethyl ester (Fura-2/AM; 1 mM stock in dimethyl sulfoxide) in PSS for 30 min at 37 °C and 5% CO<sub>2</sub> saturated humidity. After washing in PSS, the coverslip was fixed to the bottom of a Petri dish and the cells were observed by an upright epifluorescence Axiolab microscope (Carl Zeiss, Oberkochen, Germany), usually equipped with a Zeiss ×40 Achroplan objective (water-immersion, 2.0 mm working distance, 0.9 numerical aperture). The cells were excited alternately at 340 and 380 nm, and the emitted light was detected at 510 nm. A neutral density filter (1 or 0.3 optical density) reduced the overall intensity of the excitation light, and a second neutral density filter (optical density = 0.3) was coupled to the 380 nm filter to approach the intensity of the 340 nm light. A round diaphragm was used to increase the contrast. The excitation filters were mounted on a filter wheel (Lambda 10, Sutter Instrument, Novato, CA, USA). Custom software, working in the LINUX environment, was used to drive the camera (Extended-ISIS Camera, Photonic Science, Millham, UK) and the filter wheel, and to measure and plot on-line the fluorescence from 15–25 rectangular “regions of interest” (ROI) enclosing a corresponding number of single cells. Each ROI was identified by a number. Adjacent ROIs never superimposed.  $[\text{Ca}^{2+}]_i$  was monitored by measuring, for each ROI, the ratio of the mean fluorescence emitted at 510 nm when exciting alternatively at 340 and 380 nm [Ratio ( $F_{340}/F_{380}$ )]. An increase in  $[\text{Ca}^{2+}]_i$  causes an increase in the ratio [39,40]. Ratio measurements were performed and plotted on-line every 3 s. The experiments were performed at room temperature (22 °C).

### 2.4. Real-Time Reverse Transcription Quantitative PCR (qRT-PCR)

Total RNA was isolated from hCMEC/D3 cells (passage 33) using Trizol reagent (Thermo Fisher Scientific, Milan, Italy) according to the manufacturer’s instructions. After

DNase treatment (Turbo DNA-free™ kit, Thermo Fisher Scientific, Milan, Italy), RNA was quantified using a BioPhotometer D30 (Eppendorf, Hamburg, Germany). For cDNA synthesis, 100 ng RNA was reverse transcribed into 20 µL total volume using the iScript™ cDNA Synthesis Kit (Bio-Rad, Hercules, CA, USA). Real-time reverse transcription quantitative PCRs with specific primers, designed on an exon–intron junction using the NCBI Primer tool (<https://www.ncbi.nlm.nih.gov/tools/primer-blast/> (accessed on 3 March 2022)) [41] (Table S1) were performed using SsoFast™ EvaGreen® Supermix (Bio-Rad) on a CFX Connect Real-Time System (Bio-Rad) programmed as following: an initial step of 95 °C for 30 s, 40 cycles of 5 s at 95 °C, 5 s at 58 °C. A fluorescence reading was made at the end of each extension step. The PCR mixture consisted of 10 µL SsoFast™ EvaGreen® Supermix (Bio-Rad), 7 µL nuclease-free water, 1 µL cDNA and 1 µL of each forward and reverse primer. All primers were validated by melting curve analyses after each qRT-PCR run and determination of their efficiencies with at least four different cDNA concentrations. Gene expression was evaluated using the  $\Delta\Delta C_t$  method [42,43]. The genes actin beta (NM\_001101) and glyceraldehyde-3-phosphate dehydrogenase (GAPDH) (M17851) were used as endogenous reference for normalizing target mRNA [44]. For each sample, the  $2^{-\Delta\Delta C_t}$  value was calculated and represents the gene expression fold-change normalized to the reference gene and relative to the internal calibrator. Data are represented as mean  $\pm$  SEM of fold-change values. Statistical analysis was performed using log-transformed values of the raw  $2^{-\Delta\Delta C_t}$  data. The statistical comparison of fold-changes in gene expression was analyzed with a one-way analysis of variance (ANOVA) followed by Bonferroni's post-hoc test.

### 2.5. SDS-PAGE and Immunoblotting

hCMEC/D3 cells were lysed with Lysis Buffer (50 mM Tris–HCl, 150 mM NaCl, 1% Nonidet P-40, 1 mM EDTA, 0.25% deoxycholic acid, 0.1% SDS, pH 7.4, 1 mM PMSF, 5 µg/mL leupeptin, and 5 µg/mL aprotinin). Then, 10 µg of total cell proteins was separated by SDS-PAGE and transferred to a PVDF membrane. Membrane probing was performed using the different antibodies diluted 1:1000 in TBS (20 mM Tris, 500 mM NaCl, pH 7.5) containing 5% BSA and 0.1% Tween-20 in combination with the appropriate HRP-conjugated secondary antibodies (1:2000 in PBS plus 0.1% Tween-20). The following antibodies were used: anti-GABA A Receptor  $\alpha 1$ , clone 3H10 (ZRB1626) from Sigma-Aldrich (Saint Louis, MO, USA), anti-GABA B Receptor 1, clone 2D7 (ab55051) from Abcam (Cambridge, UK). The chemiluminescence reaction was performed using Immobilon Western (Millipore) and images were acquired by the Chemidoc XRS (Bio-Rad, Segrate, MI, Italy).

### 2.6. Electrophysiological Recordings

The presence of GABA<sub>A</sub>-receptor-mediated Cl<sup>−</sup> currents was assessed by using a port-a-patch planar patch-clamp system (Nanion Technologies, Munich, Germany) in the whole-cell, voltage-clamp configuration, at room temperature (22 °C), as described in [45]. Cultured cells (2–3 days after plating) were detached with Detachin and suspended at a cell density of  $1\text{--}5 \times 10^6$  cells/mL in an external recording solution containing (in mM): 145 NaCl, 2.8 KCl, 2 MgCl<sub>2</sub>, 10 CaCl<sub>2</sub>, 10 HEPES, 10 D-glucose (pH = 7.4). Suspended cells were placed on the NPC© chip surface, and the whole cell configuration was achieved. Internal recording solution, containing (in mM) 10 CsCl, 110 CsF, 10 NaCl, 10 HEPES, 10 EGTA (pH = 7.2, adjusted with CsOH), was deposited in recording chips, having resistances of 3–5 M $\Omega$ . To test the ability of GABA<sub>A</sub> receptors to conduct inward Cl<sup>−</sup> currents, 100 µM GABA or 30 µM muscimol was added to the external solution. The bioelectrical response to agonist stimulation was recorded in the voltage-clamp mode at a holding potential of −70 mV, as described in [17], by using an EPC-10 patch-clamp amplifier (HEKA, Munich, Germany). Immediately after the whole-cell configuration was established, the cell capacitance and the series resistances (<10 M $\Omega$ ) were measured. During the recordings, these two parameters were measured, and if exceeding  $\geq 10\%$  with respect to the initial value, the experiment was discontinued [45]. Liquid junction potential and



capacitive currents were cancelled using the automatic compensation of the EPC-10 [46]. Data were filtered at 10 kHz and sampled at 5 kHz.

### 2.7. Statistical Analysis of $Ca^{2+}$ Signals

All the data have been obtained from hCMEC/D3 cells from at least three independent experiments. The amplitude of agonist-evoked  $Ca^{2+}$  signals was measured as the difference between the ratio at the  $Ca^{2+}$  peak and the mean ratio of 30 s baseline before the peak. Pooled data are given as mean  $\pm$  SEM, while the number of cells analyzed is indicated above the corresponding histogram bars (number of responding cells/total number of analyzed cells). Comparisons between the two groups were done using the Student's *t*-test, whereas multiple comparisons were performed using ANOVA with the Bonferroni and Dunnett's post-hoc test, as appropriate. The Bonferroni post-hoc test was used to evaluate multiple comparisons between different means, while Dunnett's post-hoc test was used to compare each mean to a control mean. *p*-values less than 0.05 were considered statistically significant.

### 2.8. Chemicals

Fura-2/AM was purchased from Molecular Probes (Molecular Probes Europe BV, Leiden, The Netherlands). Nigericin, NED-19, NED-K, and GABA were obtained from Tocris (Bristol, UK). BTP-2 was purchased from Merck Millipore (Darmstadt, Germany). All the other chemicals were of analytical grade and obtained from Sigma Chemical Co. (St. Louis, MO, USA).

## 3. Results

### 3.1. $GABA_A$ and $GABA_B$ Receptors Are Expressed in hCMEC/D3 Cells

A thorough qRT-PCR analysis was carried out to assess whether and which GABA receptor subunits are expressed in hCMEC/D3 cells, as previously shown in mouse brain cerebrovascular endothelial cells [17,18], by using the specific primers reported in Table S1. The transcripts encoding for the following  $GABA_A$  receptor subunits were expressed:  $\alpha 1$ ,  $\alpha 5$ ,  $\beta 1$ ,  $\beta 2$ , and  $\gamma 1$  (Figure 1A). Comparison of the mean fold-change values revealed the following mRNA expression profile:  $\alpha 1 > \beta 1 > \alpha 5 = \beta 2 = \gamma 1$  (Figure 1A).  $GABA_{B1}$  and  $GABA_{B2}$  subunit mRNAs were also expressed (Figure 1B), although the transcripts encoding for the  $GABA_{B1}$  isoform were significantly up-regulated as compared to  $GABA_{B2}$  (Figure 1B). Immunoblotting confirmed that both  $GABA_A$   $\alpha 1$  and  $GABA_{B1}$  subunits were expressed at the protein level (Figure 1C). These data, therefore, demonstrate that GABA receptors are expressed also in the human cerebrovascular endothelial cell line, hCMEC/D3.

### 3.2. GABA Induces a Dose-Dependent Increase in $[Ca^{2+}]_i$ in hCMEC/D3 Cells

In order to assess whether GABA was able to increase the  $[Ca^{2+}]_i$ , hCMEC/D3 cells were loaded with the  $Ca^{2+}$ -sensitive fluorophore, Fura-2/AM, as described in [35,37]. GABA was found to induce an elevation in  $[Ca^{2+}]_i$  already at a dose as low as 1 pM (Figure 2A). The  $Ca^{2+}$  response was consistently observed by challenging hCMEC/D3 cells with increasing concentrations of GABA, ranging from 1 pM to 100  $\mu$ M (Figure 2A,B). At each dose tested, the  $Ca^{2+}$  signal comprised an initial  $Ca^{2+}$  peak which decayed to a plateau level that was maintained as long as the agonist was presented to the cells, as shown for the  $Ca^{2+}$  response to 100  $\mu$ M GABA (Figure 2C). Figure 2C shows that, after a short washout, hCMEC/D3 cells were able to promptly respond to a second application of 100  $\mu$ M GABA. The dose–response relationship did not show the typical S-shaped curve that is mediated by membrane receptors coupled to PLC; accordingly, the amplitude of the initial  $Ca^{2+}$  transient was relatively constant between 1 pM and 100 nM (Figure 2B). The highest  $Ca^{2+}$  response was elicited by 1  $\mu$ M GABA, although a robust increase in  $[Ca^{2+}]_i$  could also be observed at higher agonist concentrations, i.e., 10 and 100  $\mu$ M (Figure 2A,B). Nevertheless, 100  $\mu$ M is the concentration range that has been exploited by most of the studies investigating how GABA induced intracellular  $Ca^{2+}$  signals in neurons and astrocytes [9–13]. Furthermore,

GABA concentrations at the synaptic cleft can increase up to 80  $\mu\text{M}$  during neuronal activity [47], although they can reach over-saturating levels ( $\approx 3 \text{ mM}$ ) in response to tetanic stimulation [48]. Therefore, 100  $\mu\text{M}$  GABA, which reliably induces robust elevations in  $[\text{Ca}^{2+}]_i$  in hCMEC/D3 cells, was chosen to characterize the underlying signaling pathways.

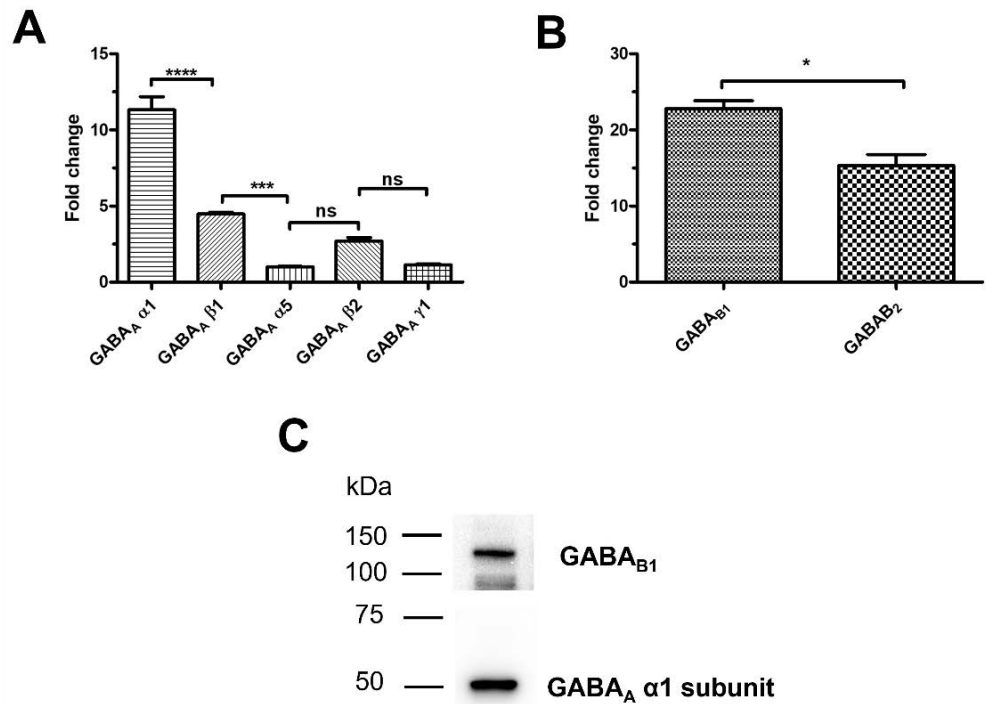


**Figure 1.** GABA<sub>A</sub> and GABA<sub>B</sub> receptors are expressed in hCMEC/D3 cells. (A), a panel of GABA<sub>A</sub> receptor subunit transcripts are expressed in hCMEC/D3 cells based on qRT-PCR data. \*\*\*\* indicate  $p < 0.0001$  \*\*\* indicate  $p < 0.001$  (One-way ANOVA followed by the post-hoc Bonferroni test). NS indicates not significant. (B), both GABA<sub>B</sub>1 and GABA<sub>B</sub>2 receptor subunit transcripts are expressed in hCMEC/D3 cells. \* indicates  $p < 0.05$  (Student's *t*-test). (C), representative immunoblots showing that both GABA<sub>A</sub>  $\alpha$ 1 and GABA<sub>B</sub>1 subunits are expressed at protein level. qRT-PCR and immunoblotting analyses were carried out on three distinct biological replicates.

**3.3. GABA-Induced Intracellular Ca<sup>2+</sup> Signals Are Sustained by Extracellular Ca<sup>2+</sup> Entry through the SOCE Pathway in hCMEC/D3 Cells**

In order to assess whether GABA was able to increase the  $[\text{Ca}^{2+}]_i$  in hCMEC/D3 cells, we loaded the  $\text{Ca}^{2+}$  sensitive fluorophore Fura2/AM as described in [35–37]. GABA was found to elicit a  $\text{Ca}^{2+}$  elevation in hCMEC/D3 cells (Figure 2A). The  $\text{Ca}^{2+}$  response is a long-lasting one that contributes to the challenge of hCMEC/D3 cells with intracellular concentrations of  $\text{Ca}^{2+}$  ranging from 300 to 1000 nM (Figure 2A,B). At each dose tested, the  $[\text{Ca}^{2+}]_i$  (Figure 2A) is a transient peak which value is elevated to a significant level (mainly 0.001) as long as the agonist was present.  $\text{Ca}^{2+}$  then declines and stabilizes at the plateau phase. The  $\text{Ca}^{2+}$  elevation is biphasic. Elevation of  $[\text{Ca}^{2+}]_i$  that, after a transient  $\text{Ca}^{2+}$  rise, hCMEC/D3 subsequent restitution of  $[\text{Ca}^{2+}]_i$  to the perfusate is induced a second elevation of  $[\text{Ca}^{2+}]_i$  which was due to extracellular  $\text{Ca}^{2+}$  entry (Figure 3B). GABA was removed from the bath 100 s before reintroducing  $\text{Ca}^{2+}$  into the external saline to prevent the activation of second messenger-operated channels (SMOCs) as discussed elsewhere [33,35,38]. The response was relatively constant between 10 nM and 100 nM (Figure 2B). The highest  $\text{Ca}^{2+}$  response was elicited by 1  $\mu\text{M}$  GABA, although a robust increase in  $[\text{Ca}^{2+}]_i$  could also be observed at higher agonist concentrations, i.e., 10 and 100  $\mu\text{M}$  (Figure 2A,B). Nevertheless, in order to confirm that SOCE sustains GABA-induced  $\text{Ca}^{2+}$  entry, hCMEC/D3 cells were pre-treated with either Pvr6 (10  $\mu\text{M}$ ), BTP-2 (20  $\mu\text{M}$ ) or  $\text{Gd}^{3+}$  (10  $\mu\text{M}$ ), three distinct inhibitors of GABA-induced intracellular  $\text{Ca}^{2+}$  signals in neurons and astrocytes [19–23]. Furthermore, GABA concentrations at the synaptic cleft can increase up to 80  $\mu\text{M}$  during neuronal activity [47], although they can reach over-saturating levels ( $\approx 3 \text{ mM}$ ) in response to tetanic stimulation [48]. Therefore, 100  $\mu\text{M}$  GABA, which reliably induces robust elevations in  $[\text{Ca}^{2+}]_i$  in hCMEC/D3 cells, was chosen to characterize the underlying signaling pathways.

depletion in these cells [32]. The pharmacological blockade of SOCE with Pyr6 or BTP-2 suppressed GABA-evoked extracellular  $\text{Ca}^{2+}$  influx in most cells and significantly reduced the amplitude of the residual  $\text{Ca}^{2+}$  entry in the remaining ones (Figure 3D,E). In accord,  $10 \mu\text{M}$   $\text{Gd}^{3+}$ , which plugs the pore of Orai1 channels [55,56], fully abolished GABA-evoked extracellular  $\text{Ca}^{2+}$  entry (Figure 3C,D). To rule out the involvement of SMOCs in the  $\text{Ca}^{2+}$  response to GABA, we inhibited Transient Receptor Potential Vanilloid 4 (TRPV) channels, which are expressed in hCMEC/D3 cells and are sensitive to RN-1734 [57]. Supplementary Figure S1 shows that pre-treatment with RN-1734 ( $20 \mu\text{M}$ ) did not affect GABA-evoked extracellular  $\text{Ca}^{2+}$  influx. Conversely, hCMEC/D3 cells express only very low levels of TRP Canonical 7 (TRPC7) channels [32], while they lack other TRPC channel isoforms that can support agonist-dependent  $\text{Ca}^{2+}$  influx in vascular endothelial cells, such as TRPC3 and TRPC6 [26,58]. Altogether, these findings indicate that SOCE supports GABA-induced intracellular  $\text{Ca}^{2+}$  signals in hCMEC/D3 cells.

Cells 2022, 11, x FOR PEER REVIEW

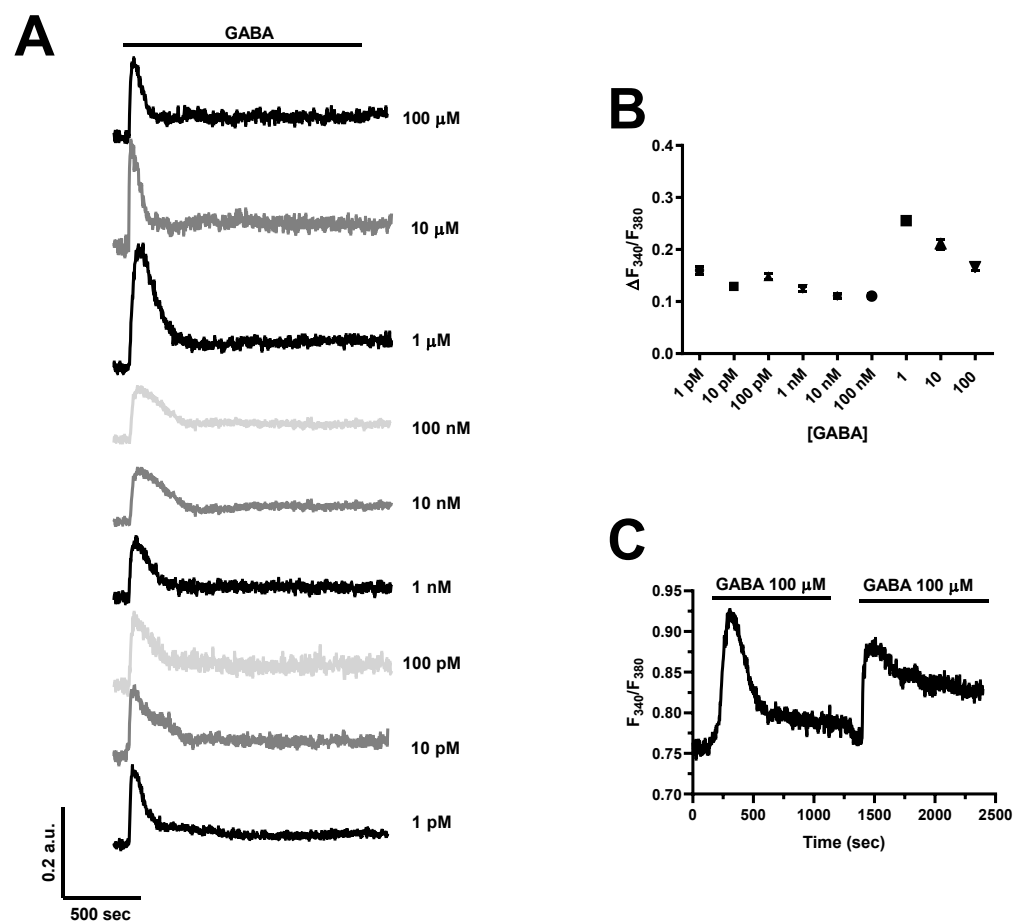


**Figure 2.** GABA evokes a dose-response increase in  $[\text{Ca}^{2+}]_i$  in hCMEC/D3 cells. (A) the inhibitory neurotransmitter, GABA, elicits a dose-dependent elevation in  $[\text{Ca}^{2+}]_i$ , which remains relatively stable between 1 pM and 100 nM and achieves its peak at 1  $\mu\text{M}$ . In this and the following figures, the black bar above the  $\text{Ca}^{2+}$  tracings indicates the time of agonist addition. (B) mean  $\pm$  SE of the amplitude of the initial  $\text{Ca}^{2+}$  peak evoked by GABA at each agonist concentration ( $[\text{GABA}]$ ). The number of analyzed cells ranges between 103 and 117 from three independent experiments for each dose. (C) GABA ( $100 \mu\text{M}$ ) elicits an additional increase in  $[\text{Ca}^{2+}]_i$  upon 3 min washout, which indicates that GABA receptors do not desensitize at this agonist concentration.

### 3.3. GABA-Induced Intracellular $\text{Ca}^{2+}$ Signals Are Sustained by Extracellular $\text{Ca}^{2+}$ Entry through the SOCE Pathway in hCMEC/D3 Cells

The endothelial  $\text{Ca}^{2+}$  response to extracellular autacoids can be shaped by extracellular  $\text{Ca}^{2+}$  entry through the plasma membrane and intracellular  $\text{Ca}^{2+}$  mobilization from endogenous organelles [26,49,50], as also demonstrated in hCMEC/D3 cells [32–36,51]. Therefore, in order to disentangle the contribution of intra- vs. extracellular  $\text{Ca}^{2+}$  sources to GABA-induced intracellular  $\text{Ca}^{2+}$  signals, we stimulated the cells in the absence of ex-

pre-treatment with RN-1734 (20  $\mu\text{M}$ ) did not affect GABA-evoked extracellular  $\text{Ca}^{2+}$  influx. Conversely, hCMEC/D3 cells express only very low levels of TRP Canonical 7 (TRPC7) channels [32], while they lack other TRPC channel isoforms that can support agonist-dependent  $\text{Ca}^{2+}$  influx in vascular endothelial cells, such as TRPC3 and TRPC6 [26,58]. Altogether, these findings indicate that SOCE supports GABA-induced intracellular  $\text{Ca}^{2+}$  signals in hCMEC/D3 cells.

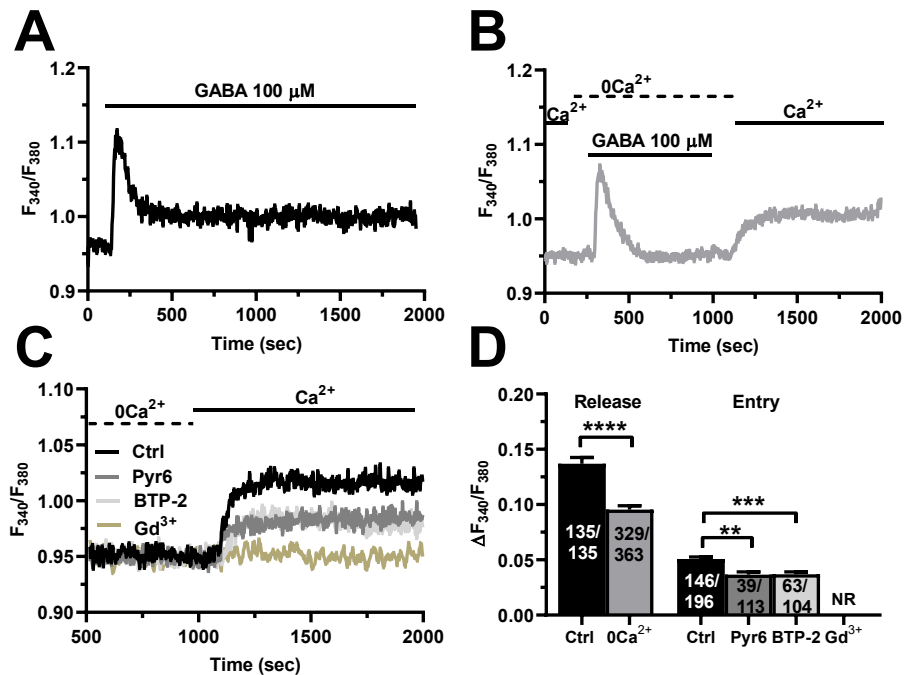


**Figure 3.** GABA evokes intracellular  $\text{Ca}^{2+}$  release and SOCE activation in hCMEC/D3 cells. (A), representative tracing of the biphasic  $\text{Ca}^{2+}$  response induced by GABA (100  $\mu\text{M}$ ) in the presence of extracellular  $\text{Ca}^{2+}$  (Ctrl). (B), representative tracing of the two distinct components of GABA-evoked intracellular  $\text{Ca}^{2+}$  signals in hCMEC/D3 cells. GABA induced a transient increase in  $[\text{Ca}^{2+}]_i$  in the absence of extracellular  $\text{Ca}^{2+}$  ( $0\text{Ca}^{2+}$ ), which is due to endogenous  $\text{Ca}^{2+}$  mobilization. Restoration of extracellular  $\text{Ca}^{2+}$  (1.5 mM) after removal of the agonist induced a second increase in  $[\text{Ca}^{2+}]_i$ , which is indicative of SOCE activation. (C), GABA-evoked extracellular  $\text{Ca}^{2+}$  entry was significantly reduced in the presence of Pyr6 (10  $\mu\text{M}$ ), BTP-2 (10  $\mu\text{M}$ ), or  $\text{Gd}^{3+}$  (20  $\mu\text{M}$ ), but not in the presence of thapsigargin (10  $\mu\text{M}$ ). Intracellular  $\text{Ca}^{2+}$  release is not shown. (D), Mean  $\pm$  SE of the amplitude of GABA-evoked  $\text{Ca}^{2+}$  peaks in the presence (Ctrl) and absence ( $0\text{Ca}^{2+}$ ) of extracellular  $\text{Ca}^{2+}$ . \*\*\*\* indicate  $p < 0.0001$  (Student's *t*-test). Mean  $\pm$  SE of the amplitude of GABA-evoked extracellular  $\text{Ca}^{2+}$  entry in the absence (Ctrl) and presence of Pyr6, BTP-2 or  $\text{Gd}^{3+}$ . \*\*\* indicate  $p < 0.001$  and \*\* indicate  $p < 0.01$  (one-way ANOVA followed by the post-hoc Dunnett's test). NR indicates "No Response" as evaluated in 89 cells from three different experiments.

### 3.4. *InsP<sub>3</sub>* and Nicotinic Acid Adenine Dinucleotide Phosphate (NAADP) Trigger GABA-Induced Intracellular $\text{Ca}^{2+}$ Release in hCMEC/D3 Cells

Growing evidence indicates that neurotransmitters and neuromodulators elicit intracellular  $\text{Ca}^{2+}$  release in the hCMEC/D3 cell line that is triggered by  $\text{InsP}_3$ -induced ER  $\text{Ca}^{2+}$  mobilization through  $\text{InsP}_3\text{Rs}$  and supported by NAADP-dependent lysosomal  $\text{Ca}^{2+}$  release via TPCs [35–37]. In accord, GABA-evoked intracellular  $\text{Ca}^{2+}$  mobilization was suppressed by blocking PLC $\beta$  activity with the aminosteroid U73122 (10  $\mu\text{M}$ ) [32,35–37] (Figure 4A) and by inhibiting  $\text{InsP}_3\text{Rs}$  with the non-competitive antagonist 2-aminoethoxydiphenyl borate (2-APB; 50  $\mu\text{M}$ ) [32,35–37] (Figure 4A). Furthermore, the endogenous  $\text{Ca}^{2+}$  response to GABA was repressed by depleting the ER  $\text{Ca}^{2+}$  store with cyclopiazonic acid (CPA; 30  $\mu\text{M}$ ) (Figure 4B), which selectively affects the sarco-endoplasmic reticulum  $\text{Ca}^{2+}$  ATPase (SERCA) activity [32,35–37]. The statistical analysis of these experiments has been reported in Figure 4C. Lysosomal  $\text{Ca}^{2+}$  release via TPCs can recruit juxtaposed  $\text{InsP}_3\text{Rs}$  through the mechanism of  $\text{Ca}^{2+}$ -induced  $\text{Ca}^{2+}$  release, thereby triggering the  $\text{Ca}^{2+}$  response to extracellular stimuli in hCMEC/D3 cells [35–37], as well as in other endothelial cell types [59]. Figure 4D shows that GABA-induced intracellular  $\text{Ca}^{2+}$  release was abrogated by depleting the lysosomal  $\text{Ca}^{2+}$  pool with nigericin (50  $\mu\text{M}$ ), which acts as a  $\text{H}^+/\text{K}^+$  antiporter and thereby dissipates the  $\text{H}^+$  gradient that maintains lysosomal  $\text{Ca}^{2+}$  refilling [60–62]. More-



over, the endogenous  $Ca^{2+}$  response to GABA (100  $\mu M$ ) was strongly inhibited by two specific NAADP antagonists, NED-19 (100  $\mu M$ ) (Figure 4E) and its chemically modified analogue, NED-K (100  $\mu M$ ) (Figure 4E) [60,63]. The analysis of these results has been illustrated in Figure 4F. Taken together, these findings demonstrate that  $InsP_3$ -induced ER  $Ca^{2+}$  release and NAADP-evoked lysosomal  $Ca^{2+}$  discharge shape GABA-evoked intracellular  $Ca^{2+}$  mobilization in hCMEC/D3 cells.

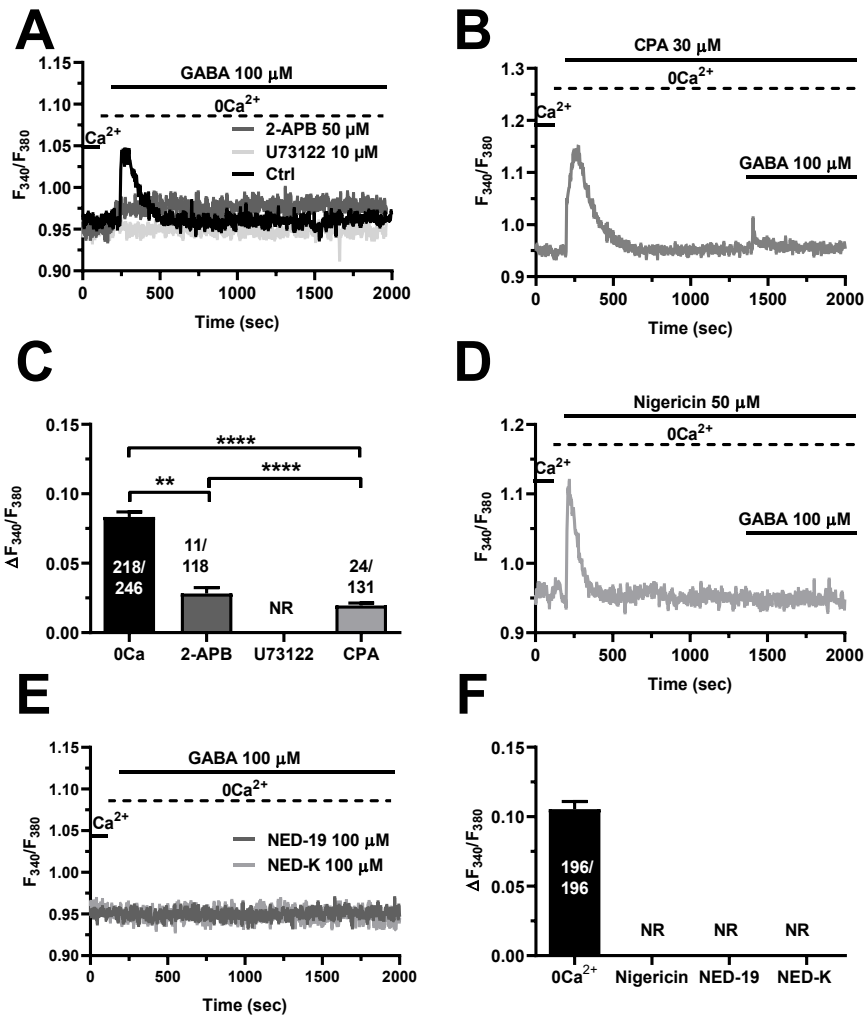


**Figure 4.**  $InsP_3$  and NAADP mediate GABA-evoked intracellular  $Ca^{2+}$  release in hCMEC/D3 cells. (A) representative tracings of GABA-evoked intracellular  $Ca^{2+}$  release in the absence (Ctrl) and presence of U73122 (10  $\mu M$ , 10 min) or 2-APB (50  $\mu M$ , 30 min), which, respectively, inhibit PLC and  $InsP_3$ . GABA was administered at 100  $\mu M$ . (B) CPA (30  $\mu M$ ), a selective blocker of SERCA activity, induced a transient elevation in  $[Ca^{2+}]_i$  under 0Ca<sup>2+</sup> conditions due to passive ER  $Ca^{2+}$  efflux. The subsequent addition of GABA (100  $\mu M$ ) induced only a small  $Ca^{2+}$  transient, which was due to the lower ER  $Ca^{2+}$  content. (C) mean  $\pm$  SE of the peak amplitude of GABA-evoked intracellular  $Ca^{2+}$  release under the designated treatments. \*\*\*\* indicate  $p < 0.0001$ , \*\*\* indicate  $p < 0.001$  (One-way ANOVA followed by the post-hoc Bonferroni test). NR indicates “No Response” as evaluated in 102 cells from three different experiments. (D) depleting the lysosomal  $Ca^{2+}$  pool with the selective H<sup>+</sup>/K<sup>+</sup> antiporter, nigericin (50  $\mu M$ ), caused a transient elevation in  $[Ca^{2+}]_i$ . The following addition of GABA (100  $\mu M$ ) induced only a small  $Ca^{2+}$  transient. (E) elevation of NAADP by GABA (100  $\mu M$ ) and NED-19 (100  $\mu M$ ) or NED-K (100  $\mu M$ ) inhibited the  $Ca^{2+}$  signal. (F) inhibition of NAADP by GABA (100  $\mu M$ ) (F) mean  $\pm$  SE of the peak amplitude of GABA-evoked intracellular  $Ca^{2+}$  release under the designated treatments. NR indicates “No Response” as evaluated in 104 cells treated with nigericin, with 101 cells treated with NED-19 and 99 cells treated with NED-K. **3.5. GABA<sub>A</sub> and GABA<sub>B</sub> Receptors Mediate GABA-Induced Intracellular  $Ca^{2+}$  Signals in hCMEC/D3 Cells**

Recent work showed that GABA<sub>A</sub> receptors initiate the  $Ca^{2+}$  response to GABA in mouse cerebrovascular endothelial cells [17]. However, GABA<sub>B</sub> receptors, which trigger an increase in  $[Ca^{2+}]_i$  in both neurons [9,10] and astrocytes [12,13], were recently found to mediate intracellular  $Ca^{2+}$  signals also in human aortic endothelial cells (HAECs) [64]. To

3.5. GABA<sub>A</sub> and GABA<sub>B</sub> Receptors Mediate GABA-Induced Intracellular Ca<sup>2+</sup> Signals in hCMEC/D3 Cells

Cells 2022, 11, x FOR PEER REVIEW

11 of 23

Recent work showed that GABA<sub>A</sub> receptors initiate the Ca<sup>2+</sup> response to GABA in mouse cerebrovascular endothelial cells [17]. However, GABA<sub>B</sub> receptors, which trigger an increase in [Ca<sup>2+</sup>]<sub>i</sub> in both neurons [9,10] and astrocytes [12,13], were recently found to mediate intracellular Ca<sup>2+</sup> signals also in human aortic endothelial cells (HAECs) [64]. To disentangle the GABA receptors involved in the endothelial Ca<sup>2+</sup> signals (Figure 5A), we first exploited a battery of selective inhibitors of GABA<sub>A</sub> and GABA<sub>B</sub> receptors. Blocking GABA<sub>A</sub> receptors with SR95531 (gabazine; 10 μM) strongly reduced the percentage of responding cells and significantly reduced the peak Ca<sup>2+</sup> response in the minority of hCMEC/D3 cells displaying a detectable Ca<sup>2+</sup> signal [22] (Figure 5B,D,E). The same inhibitory effects were achieved by selectively inhibiting GABA<sub>B</sub> receptors with the allosteric inhibitor CGP 35348 (100 μM) (Figure 5C,E). The GABA<sub>A</sub> receptors were demonstrated to be both (200 μM) or CGP 35348 (100 μM) (Figure 5C,E). The Ca<sup>2+</sup> response to GABA in hCMEC/D3 cells that both GABA<sub>A</sub> and GABA<sub>B</sub> receptors mediate the Ca<sup>2+</sup> response to GABA in hCMEC/D3 cells.

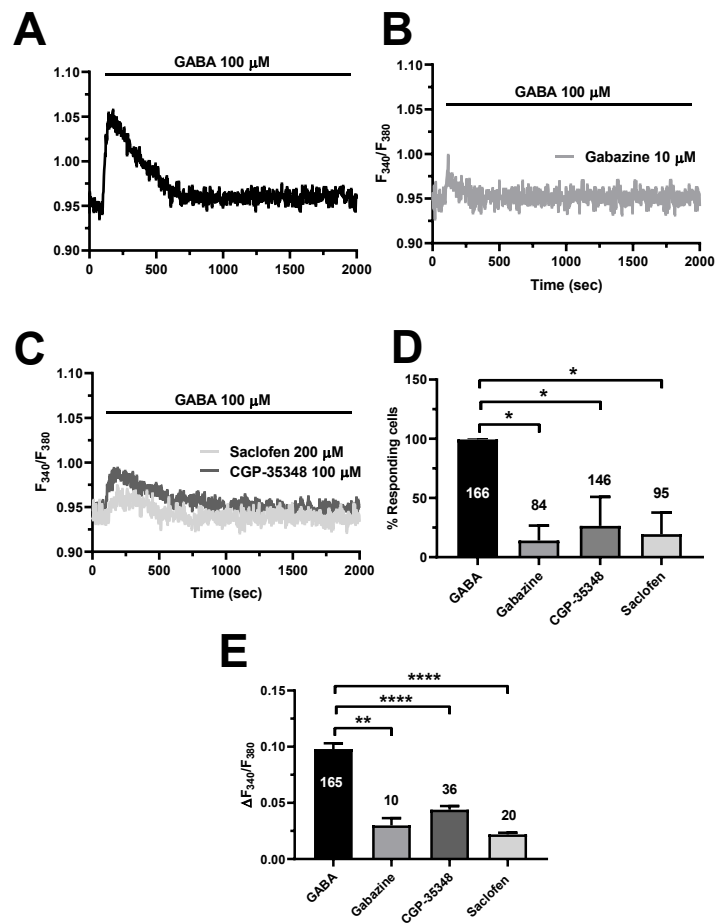


**Figure 5.** The pharmacological blockade of GABA<sub>A</sub> and GABA<sub>B</sub> receptors inhibit GABA-evoked intracellular Ca<sup>2+</sup> signals in hCMEC/D3 cells. (A) representative tracing of the Ca<sup>2+</sup> response induced by GABA (100 μM) under control (Ctrl) conditions. (B) blocking GABA<sub>A</sub> receptors with gabazine (10 μM, 5 min) significantly reduced GABA-evoked intracellular Ca<sup>2+</sup> signals. (C) blocking GABA<sub>B</sub> receptors with either saclofen (200 μM, 5 min) or CGP-35348 (100 μM, 5 min) significantly reduced GABA-evoked intracellular Ca<sup>2+</sup> signals. (D) mean ± SE of the percentage of hCMEC/D3 cells responding to GABA under the designated treatments. \* indicates p < 0.05 (one-way ANOVA followed by the post-hoc Dunnett's test). (E) mean ± SE of the amplitude of the peak Ca<sup>2+</sup> response to GABA under the designated treatments. \*\*\*\* indicates p < 0.0001, \*\*\* indicates p < 0.001, \*\* indicates p < 0.01 (one-way ANOVA followed by the post-hoc Dunnett's test).

To further corroborate these findings, we took advantage of two different agonists of GABA<sub>A</sub> and GABA<sub>B</sub> receptors, i.e., respectively, muscimol [17,22] and baclofen [12,13,22]. Figure 6A shows that both muscimol (15 μM) and baclofen (100 μM) induced a biphasic increase in [Ca<sup>2+</sup>]<sub>i</sub> that closely resembled the Ca<sup>2+</sup> response to GABA (100 μM). There was



(15  $\mu\text{M}$ ) was significantly inhibited by blocking GABA<sub>A</sub> receptors with gabazine (10  $\mu\text{M}$ ) (Figure 7D,E). Notably, muscimol-evoked intracellular Ca<sup>2+</sup> signals in hCMEC/D3 cells were also strongly reduced by inhibiting GABA<sub>B</sub> receptors with either saclofen (200  $\mu\text{M}$ ) or CGP-35348 (100  $\mu\text{M}$ ) (Figure 7D,E). Therefore, GABA<sub>A</sub> receptors require functional GABA<sub>B</sub> receptors to signal the increase in [Ca<sup>2+</sup>]<sub>i</sub> in a flux-independent manner. Similarly, the Ca<sup>2+</sup> response to baclofen (100  $\mu\text{M}$ ) was sensitive to the pharmacological blockade of either GABA<sub>A</sub> receptors with gabazine (10  $\mu\text{M}$ ) (Figure 7F,G) or GABA<sub>B</sub> receptors with saclofen (200  $\mu\text{M}$ ) and CGP-35348 (100  $\mu\text{M}$ ) (Figure 7F,G). Therefore, the sequence of signaling events leading to GABA<sub>A</sub> induced intracellular Ca<sup>2+</sup> signals in hCMEC/D3 cells requires the functional interaction between both GABA<sub>A</sub> and GABA<sub>B</sub> receptors operating in a non-canonical (i.e., flux-independent) manner via GABA<sub>A</sub> receptors operating in a non-canonical (i.e., flux-independent) manner via GABA<sub>B</sub> receptors.

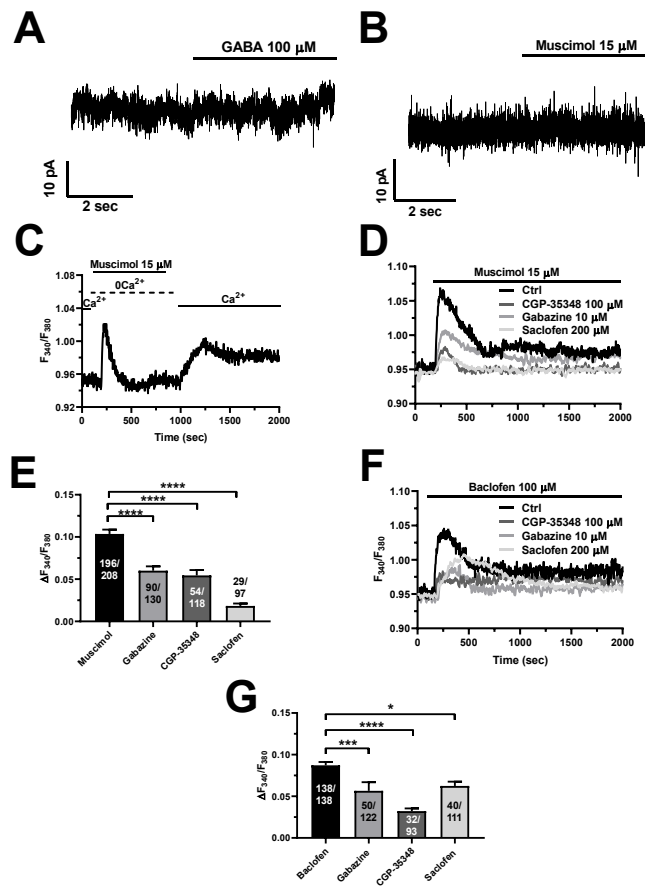


**Figure 7.** GABA-evoked intracellular Ca<sup>2+</sup> signals require the functional interaction between GABA<sub>A</sub> and GABA<sub>B</sub> receptors in hCMEC/D3 cells. Planar whole-cell patch-clamp recordings revealed that neither GABA (100  $\mu\text{M}$ ) (A) nor muscimol (15  $\mu\text{M}$ ) (B) induced any inward current at a V<sub>h</sub> = −70 mV. (C) the Ca<sup>2+</sup> add-back protocol showed that muscimol (15  $\mu\text{M}$ ) was able to mobilize the intracellular Ca<sup>2+</sup> pool under zero Ca<sup>2+</sup> conditions and to activate SOCE on restoration of extracellular Ca<sup>2+</sup> levels (1.5  $\mu\text{M}$ ) in the absence of the agonist. (D) the Ca<sup>2+</sup> response to muscimol (15  $\mu\text{M}$ ) was reduced by blocking either GABA<sub>A</sub> receptors with gabazine (10  $\mu\text{M}$ , 5 min) or GABA<sub>B</sub> receptors with saclofen (200  $\mu\text{M}$ , 5 min) or CGP-35348 (100  $\mu\text{M}$ , 5 min). (E) mean ± SE of the amplitude of the peak Ca<sup>2+</sup> response to muscimol in the absence (Ctrl) or in the presence of gabazine, CGP-35348 or baclofen (200  $\mu\text{M}$ , 5 min) or CGP-35348 (100  $\mu\text{M}$ , 5 min). (F) mean ± SE of the amplitude of the peak Ca<sup>2+</sup> response to baclofen (100  $\mu\text{M}$ ) was reduced by blocking either GABA<sub>A</sub> receptors with gabazine (10  $\mu\text{M}$ , 5 min), or GABA<sub>B</sub> receptors with saclofen (200  $\mu\text{M}$ , 5 min) or CGP-35348 (100  $\mu\text{M}$ , 5 min). (G) mean ± SE of the amplitude of the peak Ca<sup>2+</sup> response to baclofen in the absence (Ctrl) or in the presence of gabazine, CGP-35348 or saclofen. \*\*\*\* indicate  $p < 0.0001$  (one-way ANOVA followed by the post-hoc Dunnett's test). (F), the Ca<sup>2+</sup> response to baclofen (100  $\mu\text{M}$ ) was reduced by blocking either GABA<sub>A</sub> receptors with gabazine (10  $\mu\text{M}$ , 5 min), or GABA<sub>B</sub> receptors with saclofen (200  $\mu\text{M}$ , 5 min) or CGP-35348 (100  $\mu\text{M}$ , 5 min). (G), \*\*\*\* indicate  $p < 0.0001$  (one-way ANOVA followed by the post-hoc Dunnett's test). (F), the Ca<sup>2+</sup> response to baclofen (100  $\mu\text{M}$ ) was reduced by blocking either GABA<sub>A</sub> receptors with gabazine (10  $\mu\text{M}$ , 5 min), or GABA<sub>B</sub> receptors with saclofen (200  $\mu\text{M}$ , 5 min) or CGP-35348 (100  $\mu\text{M}$ , 5 min). (G), mean ± SE of the amplitude of the peak Ca<sup>2+</sup> response to baclofen in the absence (Ctrl) or in the presence of gabazine, CGP-35348 or saclofen. \*\*\*\* indicate  $p < 0.0001$ , \*\*\* indicate  $p < 0.001$ , \* indicates  $p < 0.05$  (one-way ANOVA followed by the post-hoc Dunnett's test).



To further confirm this hypothesis, we pretreated hCMEC/D3 cells with pertussis toxin (PTX), which blocks the heterotrimeric  $G_{i/o}$  proteins that recruit PLC $\beta$  upon GABA $_B$  receptor activation [10,12,22]. Figure 8 shows that PTX (1 ng/mL) significantly reduced the  $Ca^{2+}$  response to GABA $_A$  (100  $\mu$ M), muscimol (15  $\mu$ M), or baclofen (100  $\mu$ M). These findings confirm that GABA $_B$  receptors signal the increase in  $[Ca^{2+}]_i$  via G-proteins and lend further support to the view that GABA $_B$  receptors are also crucial to the onset of GABA $_A$ -receptor-mediated  $Ca^{2+}$  signals.

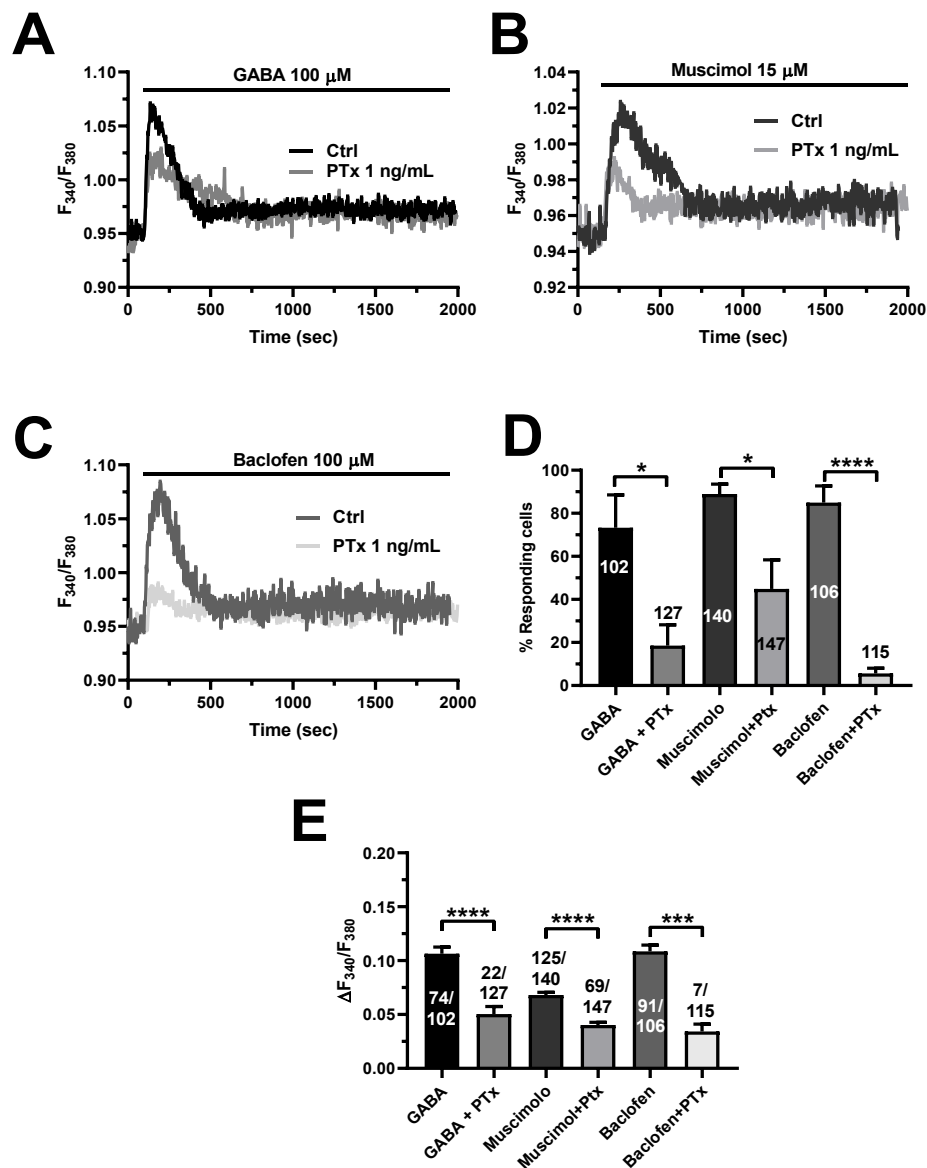


**Figure 8.** Selective inhibition of heterotrimeric  $G_{i/o}$  proteins with pertussis toxin (PTX) reduces GABA $_A$ - and GABA $_B$ -induced intracellular  $Ca^{2+}$  signals in hCMEC/D3 cells. (A), representative tracings of the biphasic  $Ca^{2+}$  signals induced by GABA (100  $\mu$ M), in the presence and in the absence of PTX (1 ng/mL). (B), Representative traces of the  $Ca^{2+}$  response induced by the GABA $_A$  receptor agonist, muscimol (15  $\mu$ M), in the presence and in the absence of PTX (1 ng/mL). (C), Representative  $Ca^{2+}$  traces evoked by the GABA $_B$  receptor agonist, baclofen (100  $\mu$ M), in the presence and in the absence of PTX (1 ng/mL). (D), mean  $\pm$  SE of the percentage of hCMEC/D3 cells responding under the designated treatments. \*\*\*\* indicate  $p < 0.0001$ , \*\*\* indicate  $p < 0.001$ , \* indicates  $p < 0.05$  (Student's *t*-test). (E), mean  $\pm$  SE of the amplitude of the peak  $Ca^{2+}$  response under the designated treatments. \*\*\*\* indicate  $p < 0.0001$ , \*\*\* indicate  $p < 0.001$ , \*\* indicate  $p < 0.01$ , \* indicates  $p < 0.05$  (Student's *t*-test).

#### 4. Discussion

Herein, we provided the first evidence that both GABA<sub>A</sub> and GABA<sub>B</sub> receptors mediate the Ca<sup>2+</sup> response to the inhibitory neurotransmitter GABA in the widely employed human cerebrovascular endothelial cell line, hCMEC/D3. We further show that GABA<sub>A</sub> receptors operate in a metabotropic, i.e., flux-independent, mode, to signal the downstream increase in [Ca<sup>2+</sup>]<sub>i</sub> via the metabotropic GABA<sub>B</sub> receptors. In line with this evidence, GABA<sub>B</sub> receptors require functional GABA<sub>A</sub> receptors to elevate the [Ca<sup>2+</sup>]<sub>i</sub> in hCMEC/D3 cells. Unravelling the molecular mechanisms involved in endothelial GABA signaling will contribute to gather further insights into the mechanisms whereby endothelial GABAergic signaling regulates the NVU.

##### 4.1. The Expression Profile of GABA<sub>A</sub> and GABA<sub>B</sub> Receptors in hCMEC/D3 Cells

The GABAergic innervation of intracortical microvessels by local GABA interneurons, rather than basal forebrain GABAergic terminals, has long been identified [15,65,66]. Subsequently, autoradiography with use of the GABA<sub>A</sub> receptor agonist, muscimol, demonstrated specific binding sites in cerebral arterioles [67]. More recently, a thorough RT-PCR characterization showed that mouse brain cerebrovascular endothelial cells express the  $\alpha 1$ ,  $\alpha 2$ ,  $\alpha 6$ ,  $\beta 1$ ,  $\beta 2$ ,  $\beta 3$ ,  $\gamma 1$ ,  $\gamma 2$  and  $\gamma 3$  subunits of GABA<sub>A</sub> receptors [18]. A similar pattern of expression has been also detected in mouse embryonic forebrain endothelial cells [17]. In the present investigation, we found that hCMEC/D3 cells express the following GABA<sub>A</sub> receptor subunits:  $\alpha 1$  (also confirmed by immunoblotting),  $\alpha 5$ ,  $\beta 1$ ,  $\beta 2$ , and  $\gamma 1$ . Therefore, human cerebrovascular endothelial cells possess all the three distinct GABA<sub>A</sub> receptor subunits that can arrange into a pentameric ion channel with the likely stoichiometry 2 $\alpha$ :2 $\beta$ :1 $\gamma$  [3,6]. Based upon their expression levels, GABA<sub>A</sub> receptors in hCMEC/D3 cells are predicted to incorporate the  $\alpha 1$ ,  $\beta 1$ , and  $\gamma 1$  subunits. Surprisingly, human cerebrovascular endothelial cells do not present the GABA<sub>A</sub> receptor  $\beta 3$  subunit, which is a crucial component of mouse GABA<sub>A</sub> receptors [17,20,21]. The expression of the GABA<sub>B</sub> receptor has hitherto been suggested only by an early study reporting on baclofen-induced nitric oxide (NO) release and collagen constriction in mouse cortical microvascular endothelial cells [19]. Herein, we provided the first evidence that both GABA<sub>B1</sub> and GABA<sub>B2</sub> subunits are expressed in hCMEC/D3 cells with GABA<sub>B1</sub> showing enriched expression. Thus, a functional GABA<sub>B</sub> receptor heterodimer can be assembled in human cerebrovascular endothelium.

##### 4.2. GABA Induces Intracellular Ca<sup>2+</sup> Signals in hCMEC/D3 Cells

GABA is emerging as a crucial mediator of neuro-to-vascular communication at the NVU [68]; mouse cerebrovascular endothelial cells express ionotropic GABA<sub>A</sub> receptors that perceive GABA released during neuronal activity from inhibitory interneurons and trigger a signaling pathway that finely controls cerebral angiogenesis [17] and CBF [20]. It has been suggested that GABA activates GABA<sub>A</sub> receptors to evoke intracellular Ca<sup>2+</sup> signals [17,20], which could, in turn, drive endothelial cell proliferation and angiogenesis [25,26,69] and recruit endothelial nitric oxide synthase (eNOS) to produce NO, i.e., the most important vaso-relaxing mediator in the brain [27,28,31,68]. Nevertheless, GABA<sub>A</sub> receptors are ionotropic receptors that are permeable to Cl<sup>-</sup> and, therefore, are not expected to directly raise the [Ca<sup>2+</sup>]<sub>i</sub> during GABAergic signaling [6]. The metabotropic GABA<sub>B</sub> receptors have recently been shown to cause a transient increase in [Ca<sup>2+</sup>]<sub>i</sub> in HAECs, but it is still unknown whether they are able to regulate the [Ca<sup>2+</sup>]<sub>i</sub> also in cerebrovascular endothelial cells. We found that GABA evoked a biphasic Ca<sup>2+</sup> response over a wide concentration range in hCMEC/D3 cells. The Ca<sup>2+</sup> response to GABA was already detectable as concentrations as low as 1 pM and achieved the peak at 1  $\mu$ M. The amplitude of the initial Ca<sup>2+</sup> peak progressively decreased with further increases in agonist concentration. This dose–response relationship is quite different from the sigmoidal curve that has been described for GABA-evoked intracellular Ca<sup>2+</sup> signals in neurons and astrocytes [70], in which the Ca<sup>2+</sup> response is exclusively mediated by the metabotropic GABA<sub>B</sub> receptors [9–13,70]. The evidence, which is further illustrated below, that the endothelial Ca<sup>2+</sup>

response to GABA is triggered by both GABA<sub>A</sub> and GABA<sub>B</sub> receptors could explain the peculiar profile of the dose–response relationship obtained in hCMEC/D3 cells. These preliminary observations confirmed that intracellular Ca<sup>2+</sup> signaling could be instrumental for GABA to control endothelial cell functions [17,20]. A novel GABA biosensor based upon a dual-enzyme immobilization approach recently showed that, during neuronal activity, GABA concentration may transiently raise up to ≈80 μM in the cortex [47]. Ca<sup>2+</sup> imaging recordings showed that 100 μM GABA elicits a robust biphasic elevation in [Ca<sup>2+</sup>]<sub>i</sub> in hCMEC/D3 cells, and this concentration was used to unveil the underlying signaling pathways. Notably, GABA-induced intracellular Ca<sup>2+</sup> waves have been observed in many cell types that do not belong to the NVU, including HAECs [64], human aortic smooth muscle cells [71], mouse embryonic stem cells [72], and the human breast cancer cell line, MCF7 [24].

#### 4.3. The Complex Mechanisms of GABA-Induced Intracellular Ca<sup>2+</sup> Signals in hCMEC/D3 Cells: InsP<sub>3</sub>Rs, TPCs and SOCE

Previous studies showed that, in neurons and astrocytes, the Ca<sup>2+</sup> response to GABA was initiated by GABA<sub>B</sub> receptors and comprised a rapid Ca<sup>2+</sup> transient that is shaped by ER Ca<sup>2+</sup> release through InsP<sub>3</sub>Rs followed by SOCE [9–13]. The PLCβ signaling pathway has been invoked also as molecular driver of GABA-induced intracellular Ca<sup>2+</sup> signals outside the NVU [24,64,71,72]. A recent series of studies demonstrated that, in hCMEC/D3 cells, the Ca<sup>2+</sup> response to neurotransmitters and neuromodulators, such as acetylcholine [32], ATP [33,34], glutamate [35,37], histamine [36] and arachidonic acid [57], is triggered by InsP<sub>3</sub>-evoked Ca<sup>2+</sup> release from the ER and maintained over time by SOCE. In addition, NAADP-induced lysosomal Ca<sup>2+</sup> discharge via TPCs can support InsP<sub>3</sub>-dependent ER Ca<sup>2+</sup> release [59,61], thereby adding a further layer of complexity to the molecular mechanisms that pattern endothelial Ca<sup>2+</sup> signals. Conversely, hCMEC/D3 cells lack ryanodine receptors [32], which may amplify InsP<sub>3</sub>-induced ER Ca<sup>2+</sup> release through the Ca<sup>2+</sup>-induced Ca<sup>2+</sup>-release (CICR) mechanism in other endothelial cell types [73].

##### 4.3.1. InsP<sub>3</sub>Rs and TPCs

Herein, pharmacological manipulation of extracellular Ca<sup>2+</sup> concentration confirmed that also the Ca<sup>2+</sup> response to GABA was dependent upon intra- and extracellular Ca<sup>2+</sup> sources. In the absence of external Ca<sup>2+</sup>, GABA evoked a smaller and transient elevation in [Ca<sup>2+</sup>]<sub>i</sub>, as previously reported in cortical neurons [9] and astrocytes [13], as well as in HAECs [64] and human aortic smooth muscle cells [71]. The GABA-evoked intracellular Ca<sup>2+</sup> release in hCMEC/D3 cells was strongly impaired by blocking PLCβ activity with U73122, by inhibiting InsP<sub>3</sub>Rs with 2-APB, and by depleting ER Ca<sup>2+</sup> content with CPA. As previously shown for acetylcholine [32], glutamate [35], ATP [33], and histamine [36], these findings convincingly indicate that InsP<sub>3</sub>-induced ER Ca<sup>2+</sup> mobilization initiates the Ca<sup>2+</sup> response to GABA in hCMEC/D3 cells. NAADP-evoked lysosomal Ca<sup>2+</sup> discharge via TPCs is emerging as a crucial mechanism shaping endothelial Ca<sup>2+</sup> signaling in peripheral vasculature [59–61,74–77]. Likewise, GABA-induced intracellular Ca<sup>2+</sup> release was disrupted by pharmacologically emptying the lysosomal Ca<sup>2+</sup> store with nigericin and by inhibiting TPCs with either NED-19 or NED-K. These results lend further support to the emerging notion that TPCs finely tune the Ca<sup>2+</sup> response to extracellular stimulation not only in cerebrovascular endothelial cells [32,35–37,57], but also in neurons and astrocytes [78–80]. It has been suggested that lysosomal Ca<sup>2+</sup> release through TPCs could trigger cytosolic CICR responses from the ER through InsP<sub>3</sub>Rs at juxtaposed ER–lysosome contact sites [61–63,81]. An alternative, but not mutually exclusive, mechanism whereby the lysosomal Ca<sup>2+</sup> store could contribute to InsP<sub>3</sub>-driven Ca<sup>2+</sup> signals is by refilling the ER with Ca<sup>2+</sup> [82]. On the other hand, InsP<sub>3</sub>-induced Ca<sup>2+</sup> release could induce the Ca<sup>2+</sup>-dependent production of NAADP [83] or favor lysosomal Ca<sup>2+</sup> loading [84], which could activate TPC2 even in the absence of its ligand [85]. Although elucidating the Ca<sup>2+</sup>-dependent cross-talk between the ER and lysosomal Ca<sup>2+</sup> stores in hCMEC/D3 cells is far beyond the

scope of the present investigation, there is no doubt that both  $\text{InsP}_3\text{Rs}$  and  $\text{TPCs}$  contribute to GABA-evoked intracellular  $\text{Ca}^{2+}$  release.

#### 4.3.2. SOCE

SOCE represents the  $\text{Ca}^{2+}$  entry pathway that mediates extracellular  $\text{Ca}^{2+}$  entry evoked by chemical cues in endothelial cells across the whole peripheral vasculature [25,86,87]. Likewise, also in hCMEC/D3 cells, SOCE sustains extracellular  $\text{Ca}^{2+}$  influx in response to acetylcholine [32], glutamate [35], and histamine [36]. In addition, SOCE can also be activated downstream of NMDARs, which signal in a flux-independent manner by recruiting the  $\text{PLC}\beta$  signaling pathway [37]. Herein, we found that the re-addition of external  $\text{Ca}^{2+}$  after GABA-dependent depletion of the ER  $\text{Ca}^{2+}$  stores, and in the absence of the agonist, evoked robust extracellular  $\text{Ca}^{2+}$  influx. Under these conditions, GABA is no longer bound to its membrane receptors and, therefore, it is unlikely to stimulate the production of intracellular second messengers, such as arachidonic acid [57], which are able to gate  $\text{Ca}^{2+}$ -permeable channels on the plasma membrane [32,35,38]. In agreement with these observations, blocking SOCE with either Pyr6 or BTP-2 significantly reduced or abolished GABA-evoked extracellular  $\text{Ca}^{2+}$  influx, whereas low micromolar doses of  $\text{Gd}^{3+}$  suppressed it. The different extents of SOCE inhibition between the pyrazole derivatives, Pyr6 and BTP-2, and the trivalent cation,  $\text{Gd}^{3+}$ , could be due to their distinct mechanisms of action. In accord, while  $\text{Gd}^{3+}$  directly plugs the channel pore of Orai1 protein, Pyr6 and BTP-2 are likely to interfere with Orai1 recruitment by STIM1 [55,88,89]. Of note, the pharmacological blockade of TRPV4 channels, which are also expressed in hCMEC/D3 cells [57], with RN-1734 did not affect GABA-evoked  $\text{Ca}^{2+}$  entry. This finding, therefore, extends the repertoire of neurotransmitters that impinge on SOCE to generate long-lasting  $\text{Ca}^{2+}$  signals within the NVU and raises the question as to whether SOCE is recruited by GABA also in HAECs [64], human aortic smooth muscle cells [71], mouse embryonic stem cells [72], and MCF-7 breast cancer cells [24].

#### 4.4. $\text{GABA}_A$ and $\text{GABA}_B$ Receptors Mediate GABA-Induced Intracellular $\text{Ca}^{2+}$ Signals in hCMEC/D3 Cells

Although the metabotropic  $\text{GABA}_B$  receptors are known to induce intracellular  $\text{Ca}^{2+}$  signals both within [9–11] and outside [24,64,71,72] the NVU, the increase in the  $[\text{Ca}^{2+}]_i$  whereby GABA regulates multiple endothelium-dependent functions in brain microvessels is mediated by the ionotropic  $\text{GABA}_A$  receptors [17,20].  $\text{GABA}_A$  receptor activation by the selective agonist muscimol elicits an inward  $\text{Cl}^-$  current in mouse cerebrovascular endothelial cells, thereby elevating the  $[\text{Ca}^{2+}]_i$  [17]. A potential explanation for this finding is that GABA-induced hyperpolarization enhances the driving-force sustaining the constitutive influx of  $\text{Ca}^{2+}$  occurring in these cells [90]. If this hypothesis holds true, muscimol should not increase the  $[\text{Ca}^{2+}]_i$  in the absence of extracellular  $\text{Ca}^{2+}$ .

Preliminary experiments revealed that both  $\text{GABA}_A$  and  $\text{GABA}_B$  receptors mediate the  $\text{Ca}^{2+}$  response to GABA. In accord, GABA-evoked intracellular  $\text{Ca}^{2+}$  signals were significantly reduced by inhibiting both the ionotropic  $\text{GABA}_A$  receptors with gabazine and the metabotropic  $\text{GABA}_B$  receptors with saclofen or CGP35348. Moreover, muscimol and baclofen, which, respectively, activate  $\text{GABA}_A$  and  $\text{GABA}_B$  receptors, also elicited a biphasic  $\text{Ca}^{2+}$  response in hCMEC/D3 cells. The following pieces of evidence support the notion that the ionotropic  $\text{GABA}_A$  receptor may signal the increase in  $[\text{Ca}^{2+}]_i$  in a flux-independent (i.e., metabotropic) mode. First, whole-cell patch-clamp recordings showed that neither GABA nor muscimol evoked a sizeable membrane current in hCMEC/D3 cells. Second, the  $\text{Ca}^{2+}$  response to muscimol was sensitive to gabazine. Third, muscimol induced a robust  $\text{Ca}^{2+}$  signal also under  $0\text{Ca}^{2+}$  conditions, which demonstrates that  $\text{GABA}_A$  receptors are able to mobilize the endogenous  $\text{Ca}^{2+}$  pool and thereby can operate in a metabotropic manner [91,92]. Intriguingly, a recent investigation revealed that, in hCMEC/D3 cells, the ionotropic NMDARs do not mediate detectable non-selective cation currents, but signal increases in  $[\text{Ca}^{2+}]_i$  in a flux-independent manner by interacting with mGluR1 and



mGluR5 [37]. In agreement with our observations, a body of studies has recently showed that also GABA<sub>A</sub> receptors present metabotropic activity and can induce InsP<sub>3</sub>-dependent ER Ca<sup>2+</sup> release in MCF-7 breast cancer cells [24] and rat cortical neurons [23]. Furthermore, it has been demonstrated that GABA<sub>A</sub> receptors may transactivate the G<sub>i/o</sub> protein coupled GABA<sub>B</sub> receptors in a PTX-dependent manner and promote InsP<sub>3</sub>-dependent ER Ca<sup>2+</sup> release in mice ciliated oviductal cells [22]. Intriguingly, also in these cells, GABA<sub>A</sub> receptor stimulation with muscimol did not activate any inward Cl<sup>-</sup> current [22]. Likewise, we found that the Ca<sup>2+</sup> response to direct GABA<sub>A</sub> receptor stimulation with muscimol was hampered by blocking GABA<sub>B</sub> receptor signaling with either saclofen, CGP35348 or PTX. Unlike the oviduct [22], however, the Ca<sup>2+</sup> response to baclofen was in turn inhibited by blocking GABA<sub>A</sub> receptors with gabazine, as well as by preventing G<sub>i/o</sub> protein activation with PTX.

These findings shed light upon an unusual mode of GABAergic signaling in the cerebrovascular endothelium. The Ca<sup>2+</sup> response to GABA, which underpins GABA-induced cerebral angiogenesis [17] and the GABA-induced local increase in CBF [20], requires the functional interaction between GABA<sub>A</sub> and GABA<sub>B</sub> receptors. GABA<sub>A</sub> receptors can engage metabolic signaling via GABA<sub>B</sub> receptors, and GABA<sub>B</sub> receptors fail to generate a full Ca<sup>2+</sup> signal if GABA<sub>A</sub> receptors are inhibited. In line with these findings, GABA<sub>A</sub> and GABA<sub>B1</sub> receptors have been shown to physically interact in mice ciliated oviductal cells [22] and in rat brain lysates [93], and to co-localize at multiple synaptic and extra-synaptic sites in the brain [94]. Future work will seek to understand the molecular underpinnings of the functional interaction between GABA<sub>A</sub> and GABA<sub>B</sub> receptors in hCMEC/D3 cells. The preliminary evidence that muscimol and baclofen do not exert an additive effect (described in Figure 6C), however, strongly suggests that the PLCβ signaling pathway is engaged by only one GABA receptor isoform, which is likely to be GABA<sub>B</sub> [7,8]. This model is supported by the evidence that PTX also attenuates muscimol-evoked intracellular Ca<sup>2+</sup> signals. Since the Ca<sup>2+</sup> response to the mixture of muscimol and baclofen is lower as compared to GABA alone, we hypothesize that the two GABA receptor isoforms must somehow be “synchronized” to interact and elicit the full Ca<sup>2+</sup> response and that this requires the presence of the physiological agonist.

## 5. Conclusions

Herein, we unveiled the complex signaling pathway whereby the inhibitory neurotransmitter GABA can induce an increase in [Ca<sup>2+</sup>]<sub>i</sub> in human cerebrovascular endothelial cells. The Ca<sup>2+</sup> response to GABA is triggered by InsP<sub>3</sub>-induced ER Ca<sup>2+</sup> release and NAADP-dependent lysosomal Ca<sup>2+</sup> mobilization, whereas it is mainly maintained by SOCE (Figure 9). Both GABA<sub>A</sub> and GABA<sub>B</sub> receptors support GABA-evoked intracellular Ca<sup>2+</sup> signals (Figure 9). The ionotropic GABA<sub>A</sub> receptors signal in a flux-independent manner via the metabotropic GABA<sub>B</sub> receptors. Likewise, the full Ca<sup>2+</sup> response to GABA<sub>B</sub> receptor stimulation requires functional GABA<sub>A</sub> receptors. Endothelial Ca<sup>2+</sup> signals finely tune a myriad of vascular functions, including those regulated by GABA, such as angiogenesis and CBF control via NO release. Therefore, this study sheds novel light on the molecular mechanisms by which GABA controls endothelial signaling at the NVU.

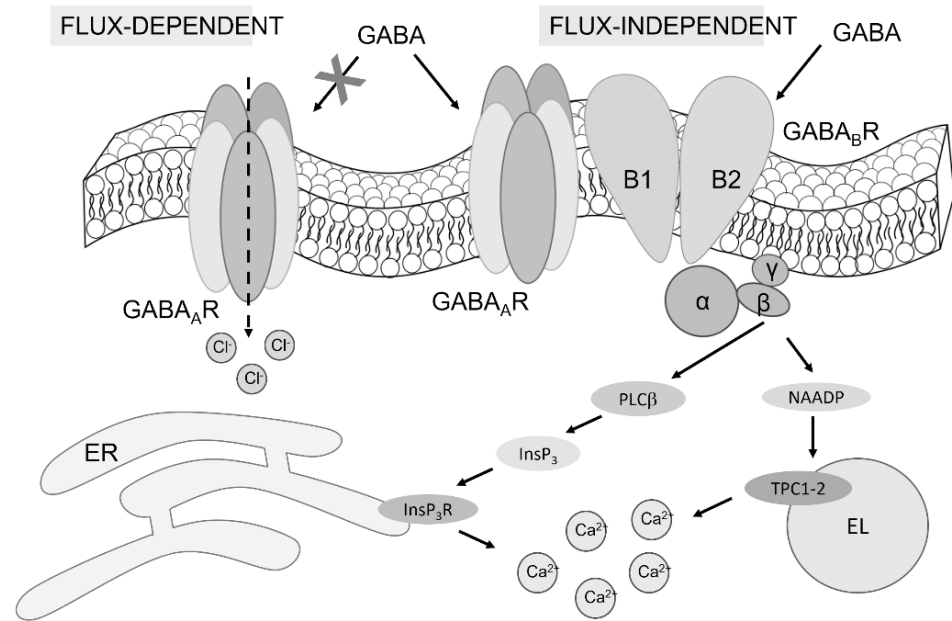


**Figure 9.** The mechanism of GABA-evoked intracellular  $\text{Ca}^{2+}$  signals in hCMEG/D3 cells. The evidence presented in this investigation demonstrates that both GABA<sub>A</sub> and GABA<sub>B</sub> receptors support the  $\text{Ca}^{2+}$  response to GABA in hCMEG/D3 cells. GABA<sub>A</sub> receptors are unlikely to signal the increase in  $[\text{Ca}^{2+}]_i$  in a flux-dependent manner, whereas they can operate in a metabotropic manner by interacting with GABA<sub>B</sub> receptors. This interaction leads to  $\text{InsP}_3$ -induced  $\text{Ca}^{2+}$  mobilization from the ER and NAADP-induced EL  $\text{Ca}^{2+}$  release through TPCs. The following reduction in ER  $\text{Ca}^{2+}$  concentrations, in turn, activates SOCE (not illustrated here).

**Supplementary Materials:** The following supporting information can be downloaded at: <https://www.mdpi.com/s1/11/11/3860/s1>. Figure S1: TPPVA inhibition does not affect GABA-evoked extracellular  $\text{Ca}^{2+}$  entry in hCMEG/D3 cells; Table S1: Primers used for real-time qPCR; Table S2: Primers used for real-time qPCR; Table S3: Primers used for real-time qPCR; Table S4: Primers used for real-time qPCR.

**Author Contributions:** Conceptualization, F.M.; methodology, S.N., F.S., M.V., V.B., P.F. and G.T.; formal analysis, S.N.; investigation, F.M., S.N., F.S., M.V., V.B., P.F. and G.T.; data curation, F.M., S.N., F.S., M.V., V.B., P.F. and G.T.; validation, F.M., S.N., F.S., M.V., V.B., P.F. and G.T.; writing original draft preparation, F.M.; writing review and editing, F.M., S.N., F.S., M.V., V.B., P.F. and G.T.; supervision, F.M.; project administration, F.M.; funding acquisition, F.M. All authors have read and agreed to the published version of the manuscript.

**Funding:** This research was funded by Regione Lombardia, regional law n° 9/2020, resolution n° 2776/2020 (F.M.); Italian Ministry of Education, University and Research (MIUR), Progetti di Ricerca di Interesse Nazionale (PRIN) 2017-2020, grant number 2017/16737 (F.M.); University of Pavia, Program of Research Projects of Biological and Biotechnology (via Galvani) and the University of Pavia (F.M.); Fonda Ricerca Giovani from the University of Pavia (F.M.); FET OPEN-2018-2020 Program under Grant Agreement N. 828984, LION-HEARTED (P.M.); 2020 FETOPEN-2018-2020 Program under Grant Agreement N. 828984, LION-HEARTED (F.M.).

**Institutional Review Board Statement:** Not applicable.

**Institutional Review Board Statement:** Not applicable.

**Informed Consent Statement:** Not applicable.

**Informed Consent Statement:** Not applicable.

**Data Availability Statement:** Data supporting reported results can be obtained by the corresponding author upon reasonable request.

**Acknowledgments:** The authors gratefully acknowledge the Laboratory of Cellular Electrophysiology, Centro Grandi Strumenti of the University of Pavia, for the use of the Port-a-Patch automated system.

**Conflicts of Interest:** The authors declare no conflict of interest.

**Conflicts of Interest:** The authors declare no conflict of interest.

## References

1. Mapelli, L.; Soda, T.; D'Angelo, E.; Prestori, F. The Cerebellar Involvement in Autism Spectrum Disorders: From the Social Brain to Mouse Models. *Int. J. Mol. Sci.* **2022**, *23*, 3894. <https://doi.org/10.3390/ijms23073894>.

## References

1. Mapelli, L.; Soda, T.; D'Angelo, E.; Prestori, F. The Cerebellar Involvement in Autism Spectrum Disorders: From the Social Brain to Mouse Models. *Int. J. Mol. Sci.* **2022**, *23*, 3894. [[CrossRef](#)] [[PubMed](#)]
2. Soda, T.; Mapelli, L.; Locatelli, F.; Botta, L.; Goldfarb, M.; Prestori, F.; D'Angelo, E. Hyperexcitability and Hyperplasticity Disrupt Cerebellar Signal Transfer in the IB2 KO Mouse Model of Autism. *J. Neurosci.* **2019**, *39*, 2383–2397. [[CrossRef](#)] [[PubMed](#)]
3. Sakimoto, Y.; Oo, P.M.; Goshima, M.; Kanehisa, I.; Tsukada, Y.; Mitsushima, D. Significance of GABAA Receptor for Cognitive Function and Hippocampal Pathology. *Int. J. Mol. Sci.* **2021**, *22*, 12456. [[CrossRef](#)] [[PubMed](#)]
4. Fukuda, A. Chloride homeodynamics underlying modal shifts in cellular and network oscillations. *Neurosci. Res.* **2020**, *156*, 14–23. [[CrossRef](#)] [[PubMed](#)]
5. Cherubini, E.; Di Cristo, G.; Avoli, M. Dysregulation of GABAergic Signaling in Neurodevelopmental Disorders: Targeting Cation-Chloride Co-transporters to Re-establish a Proper E/I Balance. *Front. Cell. Neurosci.* **2021**, *15*, 813441. [[CrossRef](#)]
6. Alexander, S.P.; Mathie, A.; Peters, J.A.; Veale, E.L.; Striessnig, J.; Kelly, E.; Armstrong, J.F.; Faccenda, E.; Harding, S.D.; Pawson, A.J.; et al. The Concise Guide to Pharmacology 2021/22: Ion channels. *Br. J. Pharmacol.* **2021**, *178* (Suppl. S1), S157–S245. [[CrossRef](#)]
7. Bassetti, D. Keeping the Balance: GABAB Receptors in the Developing Brain and Beyond. *Brain Sci.* **2022**, *12*, 419. [[CrossRef](#)]
8. Vlachou, S. A Brief History and the Significance of the GABAB Receptor. *Curr. Top. Behav. Neurosci.* **2022**, *52*, 1–17. [[CrossRef](#)]
9. New, D.C.; An, H.; Ip, N.Y.; Wong, Y.H. GABAB heterodimeric receptors promote  $Ca^{2+}$  influx via store-operated channels in rat cortical neurons and transfected Chinese hamster ovary cells. *Neuroscience* **2006**, *137*, 1347–1358. [[CrossRef](#)]
10. Kardos, J.; Elster, L.; Damgaard, I.; Krogsgaard-Larsen, P.; Schousboe, A. Role of GABAB receptors in intracellular  $Ca^{2+}$  homeostasis and possible interaction between GABAA and GABAB receptors in regulation of transmitter release in cerebellar granule neurons. *J. Neurosci. Res.* **1994**, *39*, 646–655. [[CrossRef](#)]
11. Nieto, A.; Bailey, T.; Kaczanowska, K.; McDonald, P. GABAB Receptor Chemistry and Pharmacology: Agonists, Antagonists, and Allosteric Modulators. *Curr. Top. Behav. Neurosci.* **2022**, *52*, 81–118. [[CrossRef](#)] [[PubMed](#)]
12. Mariotti, L.; Losi, G.; Sessolo, M.; Marcon, I.; Carmignoto, G. The inhibitory neurotransmitter GABA evokes long-lasting  $Ca^{2+}$  oscillations in cortical astrocytes. *Glia* **2016**, *64*, 363–373. [[CrossRef](#)] [[PubMed](#)]
13. Kang, J.; Jiang, L.; Goldman, S.A.; Nedergaard, M. Astrocyte-mediated potentiation of inhibitory synaptic transmission. *Nat. Neurosci.* **1998**, *1*, 683–692. [[CrossRef](#)] [[PubMed](#)]
14. Choi, Y.K.; Vasudevan, A. Endothelial GABA signaling: A phoenix awakened. *Aging* **2018**, *10*, 859–860. [[CrossRef](#)] [[PubMed](#)]
15. Vaucher, E.; Tong, X.K.; Cholet, N.; Lantin, S.; Hamel, E. GABA neurons provide a rich input to microvessels but not nitric oxide neurons in the rat cerebral cortex: A means for direct regulation of local cerebral blood flow. *J. Comp. Neurol.* **2000**, *421*, 161–171. [[CrossRef](#)]
16. Won, C.; Lin, Z.; Kumar, T.P.; Li, S.; Ding, L.; Elkhali, A.; Szabo, G.; Vasudevan, A. Autonomous vascular networks synchronize GABA neuron migration in the embryonic forebrain. *Nat. Commun.* **2013**, *4*, 2149. [[CrossRef](#)]
17. Li, S.; Kumar, T.P.; Joshee, S.; Kirschstein, T.; Subburaju, S.; Khalili, J.S.; Kloeppe, J.; Du, C.; Elkhali, A.; Szabo, G.; et al. Endothelial cell-derived GABA signaling modulates neuronal migration and postnatal behavior. *Cell Res.* **2018**, *28*, 221–248. [[CrossRef](#)]
18. Tyagi, N.; Lominadze, D.; Gillespie, W.; Moshal, K.S.; Sen, U.; Rosenberger, D.S.; Steed, M.; Tyagi, S.C. Differential expression of gamma-aminobutyric acid receptor A (GABA(A)) and effects of homocysteine. *Clin. Chem. Lab. Med.* **2007**, *45*, 1777–1784. [[CrossRef](#)]
19. Shastry, S.; Moning, L.; Tyagi, N.; Steed, M.; Tyagi, S.C. GABA receptors and nitric oxide ameliorate constrictive collagen remodeling in hyperhomocysteinemia. *J. Cell. Physiol.* **2005**, *205*, 422–427. [[CrossRef](#)]
20. Agrud, A.; Subburaju, S.; Goel, P.; Ren, J.; Kumar, A.S.; Caldarone, B.J.; Dai, W.; Chavez, J.; Fukumura, D.; Jain, R.K.; et al. Gabrb3 endothelial cell-specific knockout mice display abnormal blood flow, hypertension, and behavioral dysfunction. *Sci. Rep.* **2022**, *12*, 4922. [[CrossRef](#)]
21. Choi, Y.K.; Vasudevan, A. Mechanistic insights into autocrine and paracrine roles of endothelial GABA signaling in the embryonic forebrain. *Sci. Rep.* **2019**, *9*, 16256. [[CrossRef](#)] [[PubMed](#)]
22. Jung, C.; Fernandez-Duenas, V.; Plata, C.; Garcia-Elias, A.; Ciruela, F.; Fernandez-Fernandez, J.M.; Valverde, M.A. Functional coupling of GABAA/B receptors and the channel TRPV4 mediates rapid progesterone signaling in the oviduct. *Sci. Signal.* **2018**, *11*, eaam6558. [[CrossRef](#)] [[PubMed](#)]
23. Nicholson, M.W.; Sweeney, A.; Pekle, E.; Alam, S.; Ali, A.B.; Duchon, M.; Jovanovic, J.N. Diazepam-induced loss of inhibitory synapses mediated by PLCdelta/ $Ca^{2+}$ /calcineurin signalling downstream of GABAA receptors. *Mol. Psychiatry* **2018**, *23*, 1851–1867. [[CrossRef](#)] [[PubMed](#)]
24. Chen, X.; Cao, Q.; Liao, R.; Wu, X.; Xun, S.; Huang, J.; Dong, C. Loss of ABAT-Mediated GABAergic System Promotes Basal-Like Breast Cancer Progression by Activating  $Ca^{2+}$ -NFAT1 Axis. *Theranostics* **2019**, *9*, 34–47. [[CrossRef](#)]
25. Moccia, F.; Negri, S.; Shekha, M.; Faris, P.; Guerra, G. Endothelial  $Ca^{2+}$  Signaling, Angiogenesis and Vasculogenesis: Just What It Takes to Make a Blood Vessel. *Int. J. Mol. Sci.* **2019**, *20*, 3962. [[CrossRef](#)]
26. Negri, S.; Faris, P.; Berra-Romani, R.; Guerra, G.; Moccia, F. Endothelial Transient Receptor Potential Channels and Vascular Remodeling: Extracellular  $Ca^{2+}$  Entry for Angiogenesis, Arteriogenesis and Vasculogenesis. *Front. Physiol.* **2019**, *10*, 1618. [[CrossRef](#)]

27. Negri, S.; Faris, P.; Soda, T.; Moccia, F. Endothelial signaling at the core of neurovascular coupling: The emerging role of endothelial inward-rectifier K(+) (Kir2.1) channels and N-methyl-d-aspartate receptors in the regulation of cerebral blood flow. *Int. J. Biochem. Cell Biol.* **2021**, *135*, 105983. [[CrossRef](#)]
28. Guerra, G.; Lucariello, A.; Perna, A.; Botta, L.; de Luca, A.; Moccia, F. The Role of Endothelial Ca<sup>2+</sup> Signaling in Neurovascular Coupling: A View from the Lumen. *Int. J. Mol. Sci.* **2018**, *19*, 938. [[CrossRef](#)]
29. Helms, H.C.; Abbott, N.J.; Burek, M.; Cecchelli, R.; Couraud, P.O.; Deli, M.A.; Forster, C.; Galla, H.J.; Romero, I.A.; Shusta, E.V.; et al. In vitro models of the blood-brain barrier: An overview of commonly used brain endothelial cell culture models and guidelines for their use. *J. Cereb. Blood Flow Metab.* **2016**, *36*, 862–890. [[CrossRef](#)]
30. Weksler, B.; Romero, I.A.; Couraud, P.O. The hCMEC/D3 cell line as a model of the human blood brain barrier. *Fluids Barriers CNS* **2013**, *10*, 16. [[CrossRef](#)] [[PubMed](#)]
31. Moccia, F.; Negri, S.; Faris, P.; Angelone, T. Targeting endothelial ion signalling to rescue cerebral blood flow in cerebral disorders. *Vascul. Pharmacol.* **2022**, *145*, 106997. [[CrossRef](#)] [[PubMed](#)]
32. Zuccolo, E.; Laforenza, U.; Negri, S.; Botta, L.; Berra-Romani, R.; Faris, P.; Scarpellino, G.; Forcaia, G.; Pellavio, G.; Sancini, G.; et al. Muscarinic M5 receptors trigger acetylcholine-induced Ca<sup>2+</sup> signals and nitric oxide release in human brain microvascular endothelial cells. *J. Cell. Physiol.* **2019**, *234*, 4540–4562. [[CrossRef](#)] [[PubMed](#)]
33. Bintig, W.; Begandt, D.; Schlingmann, B.; Gerhard, L.; Pangalos, M.; Dreyer, L.; Hohnjec, N.; Couraud, P.O.; Romero, I.A.; Weksler, B.B.; et al. Purine receptors and Ca<sup>2+</sup> signalling in the human blood-brain barrier endothelial cell line hCMEC/D3. *Purinergic Signal.* **2012**, *8*, 71–80. [[CrossRef](#)] [[PubMed](#)]
34. Forcaia, G.; Formicola, B.; Terribile, G.; Negri, S.; Lim, D.; Biella, G.; Re, F.; Moccia, F.; Sancini, G. Multifunctional Liposomes Modulate Purinergic Receptor-Induced Calcium Wave in Cerebral Microvascular Endothelial Cells and Astrocytes: New Insights for Alzheimer's disease. *Mol. Neurobiol.* **2021**, *58*, 2824–2835. [[CrossRef](#)] [[PubMed](#)]
35. Negri, S.; Faris, P.; Pellavio, G.; Botta, L.; Orgiu, M.; Forcaia, G.; Sancini, G.; Laforenza, U.; Moccia, F. Group 1 metabotropic glutamate receptors trigger glutamate-induced intracellular Ca<sup>2+</sup> signals and nitric oxide release in human brain microvascular endothelial cells. *Cell. Mol. Life Sci.* **2020**, *77*, 2235–2253. [[CrossRef](#)]
36. Berra-Romani, R.; Faris, P.; Pellavio, G.; Orgiu, M.; Negri, S.; Forcaia, G.; Var-Gaz-Guadarrama, V.; Garcia-Carrasco, M.; Botta, L.; Sancini, G.; et al. Histamine induces intracellular Ca<sup>2+</sup> oscillations and nitric oxide release in endothelial cells from brain microvascular circulation. *J. Cell. Physiol.* **2020**, *235*, 1515–1530. [[CrossRef](#)] [[PubMed](#)]
37. Negri, S.; Faris, P.; Maniezz, C.; Pellavio, G.; Spaiardi, P.; Botta, L.; Laforenza, U.; Biella, G.; Moccia, D.F. NMDA receptors elicit flux-independent intracellular Ca<sup>2+</sup> signals via metabotropic glutamate receptors and flux-dependent nitric oxide release in human brain microvascular endothelial cells. *Cell Calcium* **2021**, *99*, 102454. [[CrossRef](#)]
38. Zuccolo, E.; Kheder, D.A.; Lim, D.; Perna, A.; Nezza, F.D.; Botta, L.; Scarpellino, G.; Negri, S.; Martinotti, S.; Soda, T.; et al. Glutamate triggers intracellular Ca<sup>2+</sup> oscillations and nitric oxide release by inducing NAADP- and InsP3 -dependent Ca<sup>2+</sup> release in mouse brain endothelial cells. *J. Cell. Physiol.* **2019**, *234*, 3538–3554. [[CrossRef](#)]
39. Gerbino, A.; Bottillo, I.; Milano, S.; Lipari, M.; Zio, R.; Morlino, S.; Mola, M.G.; Procino, G.; Re, F.; Zachara, E.; et al. Functional Characterization of a Novel Truncating Mutation in Lamin A/C Gene in a Family with a Severe Cardiomyopathy with Conduction Defects. *Cell. Physiol. Biochem.* **2017**, *44*, 1559–1577. [[CrossRef](#)]
40. Milano, S.; Gerbino, A.; Schena, G.; Carmosino, M.; Svelto, M.; Procino, G. Human beta3-Adrenoreceptor is Resistant to Agonist-Induced Desensitization in Renal Epithelial Cells. *Cell. Physiol. Biochem.* **2018**, *48*, 847–862. [[CrossRef](#)]
41. Ye, J.; Coulouris, G.; Zaretskaya, I.; Cutcutache, I.; Rozen, S.; Madden, T.L. Primer-BLAST: A tool to design target-specific primers for polymerase chain reaction. *BMC Bioinform.* **2012**, *13*, 134. [[CrossRef](#)] [[PubMed](#)]
42. Livak, K.J.; Schmittgen, T.D. Analysis of relative gene expression data using real-time quantitative PCR and the 2(-Delta Delta C(T)) Method. *Methods* **2001**, *25*, 402–408. [[CrossRef](#)] [[PubMed](#)]
43. Pfaffl, M.W. A new mathematical model for relative quantification in real-time RT-PCR. *Nucleic Acids Res.* **2001**, *29*, e45. [[CrossRef](#)]
44. Ferrera, L.; Barbieri, R.; Picco, C.; Zuccolini, P.; Remigante, A.; Bertelli, S.; Fumagalli, M.R.; Zifarelli, G.; La Porta, C.A.M.; Gavazzo, P.; et al. TRPM2 Oxidation Activates Two Distinct Potassium Channels in Melanoma Cells through Intracellular Calcium Increase. *Int. J. Mol. Sci.* **2021**, *22*, 8359. [[CrossRef](#)] [[PubMed](#)]
45. Sobradillo, D.; Hernandez-Morales, M.; Ubierna, D.; Moyer, M.P.; Nunez, L.; Villalobos, C. A reciprocal shift in transient receptor potential channel 1 (TRPC1) and stromal interaction molecule 2 (STIM2) contributes to Ca<sup>2+</sup> remodeling and cancer hallmarks in colorectal carcinoma cells. *J. Biol. Chem.* **2014**, *289*, 28765–28782. [[CrossRef](#)] [[PubMed](#)]
46. Costa, R.; Remigante, A.; Civello, D.A.; Bernardinelli, E.; Szabo, Z.; Morabito, R.; Marino, A.; Sarikas, A.; Patsch, W.; Paulmichl, M.; et al. O-GlcNAcylation Suppresses the Ion Current ICl<sub>swell</sub> by Preventing the Binding of the Protein ICl<sub>n</sub> to alpha-Integrin. *Front. Cell Dev. Biol.* **2020**, *8*, 607080. [[CrossRef](#)] [[PubMed](#)]
47. Burmeister, J.J.; Price, D.A.; Pomerleau, F.; Huettl, P.; Quintero, J.E.; Gerhardt, G.A. Challenges of simultaneous measurements of brain extracellular GABA and glutamate in vivo using enzyme-coated microelectrode arrays. *J. Neurosci. Methods* **2020**, *329*, 108435. [[CrossRef](#)]
48. Grabauskas, G. Time course of GABA in the synaptic clefts of inhibitory synapses in the rostral nucleus of the solitary tract. *Neurosci. Lett.* **2005**, *373*, 10–15. [[CrossRef](#)]
49. Negri, S.; Faris, P.; Moccia, F. Reactive Oxygen Species and Endothelial Ca<sup>2+</sup> Signaling: Brothers in Arms or Partners in Crime? *Int. J. Mol. Sci.* **2021**, *22*, 9821. [[CrossRef](#)]



50. McCarron, J.G.; Lee, M.D.; Wilson, C. The Endothelium Solves Problems That Endothelial Cells Do Not Know Exist. *Trends Pharmacol. Sci.* **2017**, *38*, 322–338. [[CrossRef](#)]
51. Bader, A.; Bintig, W.; Begandt, D.; Klett, A.; Siller, I.G.; Gregor, C.; Schaarschmidt, F.; Weksler, B.; Romero, I.; Couraud, P.O.; et al. Adenosine receptors regulate gap junction coupling of the human cerebral microvascular endothelial cells hCMEC/D3 by Ca<sup>2+</sup> influx through cyclic nucleotide-gated channels. *J. Physiol.* **2017**, *595*, 2497–2517. [[CrossRef](#)] [[PubMed](#)]
52. Zhang, X.; Xin, P.; Yoast, R.E.; Emrich, S.M.; Johnson, M.T.; Pathak, T.; Benson, J.C.; Azimi, I.; Gill, D.L.; Monteith, G.R.; et al. Distinct pharmacological profiles of ORAI1, ORAI2, and ORAI3 channels. *Cell Calcium* **2020**, *91*, 102281. [[CrossRef](#)] [[PubMed](#)]
53. Abdullaev, I.F.; Bisailon, J.M.; Potier, M.; Gonzalez, J.C.; Motiani, R.K.; Trebak, M. Stim1 and Orai1 mediate CRAC currents and store-operated calcium entry important for endothelial cell proliferation. *Circ. Res.* **2008**, *103*, 1289–1299. [[CrossRef](#)]
54. Lodola, F.; Laforenza, U.; Bonetti, E.; Lim, D.; Dragoni, S.; Bottino, C.; Ong, H.L.; Guerra, G.; Ganini, C.; Massa, M.; et al. Store-operated Ca<sup>2+</sup> entry is remodelled and controls in vitro angiogenesis in endothelial progenitor cells isolated from tumoral patients. *PLoS ONE* **2012**, *7*, e42541. [[CrossRef](#)]
55. Prakriya, M.; Lewis, R.S. Store-Operated Calcium Channels. *Physiol. Rev.* **2015**, *95*, 1383–1436. [[CrossRef](#)] [[PubMed](#)]
56. Moccia, F.; Zuccolo, E.; Poletto, V.; Turin, I.; Guerra, G.; Pedrazzoli, P.; Rosti, V.; Porta, C.; Montagna, D. Targeting Stim and Orai Proteins as an Alternative Approach in Anticancer Therapy. *Curr. Med. Chem.* **2016**, *23*, 3450–3480. [[CrossRef](#)]
57. Berra-Romani, R.; Faris, P.; Negri, S.; Botta, L.; Genova, T.; Moccia, F. Arachidonic Acid Evokes an Increase in Intracellular Ca<sup>2+</sup> Concentration and Nitric Oxide Production in Endothelial Cells from Human Brain Microcirculation. *Cells* **2019**, *8*, 689. [[CrossRef](#)]
58. Thakore, P.; Earley, S. Transient Receptor Potential Channels and Endothelial Cell Calcium Signaling. *Compr. Physiol.* **2019**, *9*, 1249–1277. [[CrossRef](#)]
59. Moccia, F.; Negri, S.; Faris, P.; Perna, A.; de Luca, A.; Soda, T.; Romani, R.B.; Guerra, G. Targeting Endolysosomal Two-Pore Channels to Treat Cardiovascular Disorders in the Novel CoronaVirus Disease 2019. *Front. Physiol.* **2021**, *12*, 629119. [[CrossRef](#)]
60. Moccia, F.; Zuccolo, E.; Di Nezza, F.; Pellavio, G.; Faris, P.S.; Negri, S.; de Luca, A.; Laforenza, U.; Ambrosone, L.; Rosti, V.; et al. Nicotinic acid adenine dinucleotide phosphate activates two-pore channel TPC1 to mediate lysosomal Ca<sup>2+</sup> release in endothelial colony-forming cells. *J. Cell. Physiol.* **2021**, *236*, 688–705. [[CrossRef](#)]
61. Negri, S.; Faris, P.; Moccia, F. Endolysosomal Ca<sup>2+</sup> signaling in cardiovascular health and disease. *Int. Rev. Cell Mol. Biol.* **2021**, *363*, 203–269. [[CrossRef](#)] [[PubMed](#)]
62. Morgan, A.J.; Platt, F.M.; Lloyd-Evans, E.; Galione, A. Molecular mechanisms of endolysosomal Ca<sup>2+</sup> signalling in health and disease. *Biochem. J.* **2011**, *439*, 349–374. [[CrossRef](#)] [[PubMed](#)]
63. Faris, P.; Casali, C.; Negri, S.; Iengo, L.; Biggiogera, M.; Maione, A.S.; Moccia, F. Nicotinic Acid Adenine Dinucleotide Phosphate Induces Intracellular Ca<sup>2+</sup> Signalling and Stimulates Proliferation in Human Cardiac Mesenchymal Stromal Cells. *Front. Cell Dev. Biol.* **2022**, *10*, 874043. [[CrossRef](#)] [[PubMed](#)]
64. Wang, X.P.; Cheng, Z.Y.; Schmid, K.L. GABAB receptors expressed in human aortic endothelial cells mediate intracellular calcium concentration regulation and endothelial nitric oxide synthase translocation. *BioMed Res. Int.* **2014**, *2014*, 871735. [[CrossRef](#)] [[PubMed](#)]
65. Hamel, E. Perivascular nerves and the regulation of cerebrovascular tone. *J. Appl. Physiol.* **2006**, *100*, 1059–1064. [[CrossRef](#)] [[PubMed](#)]
66. Cauli, B.; Tong, X.K.; Rancillac, A.; Serluca, N.; Lambolez, B.; Rossier, J.; Hamel, E. Cortical GABA interneurons in neurovascular coupling: Relays for subcortical vasoactive pathways. *J. Neurosci.* **2004**, *24*, 8940–8949. [[CrossRef](#)]
67. Napoleone, P.; Erdo, S.; Amenta, F. Autoradiographic localization of the GABAA receptor agonist [3H] muscimol in rat cerebral vessels. *Brain Res.* **1987**, *423*, 109–115. [[CrossRef](#)]
68. Kaplan, L.; Chow, B.W.; Gu, C. Neuronal regulation of the blood-brain barrier and neurovascular coupling. *Nat. Rev. Neurosci.* **2020**, *21*, 416–432. [[CrossRef](#)]
69. Moccia, F. Endothelial Ca<sup>2+</sup> Signaling and the Resistance to Anticancer Treatments: Partners in Crime. *Int. J. Mol. Sci.* **2018**, *19*, 217. [[CrossRef](#)]
70. Doengi, M.; Hirnet, D.; Coulon, P.; Pape, H.C.; Deitmer, J.W.; Lohr, C. GABA uptake-dependent Ca<sup>2+</sup> signaling in developing olfactory bulb astrocytes. *Proc. Natl. Acad. Sci. USA* **2009**, *106*, 17570–17575. [[CrossRef](#)]
71. Wang, X.P.; Cheng, Z.Y.; Schmid, K.L. GABAB receptors are expressed in human aortic smooth muscle cells and regulate the intracellular Ca<sup>2+</sup> concentration. *Heart Vessel.* **2015**, *30*, 249–257. [[CrossRef](#)]
72. Schwirtlich, M.; Emri, Z.; Antal, K.; Mate, Z.; Katarova, Z.; Szabo, G. GABA(A) and GABA(B) receptors of distinct properties affect oppositely the proliferation of mouse embryonic stem cells through synergistic elevation of intracellular Ca<sup>2+</sup>. *FASEB J.* **2010**, *24*, 1218–1228. [[CrossRef](#)] [[PubMed](#)]
73. Evangelista, A.M.; Thompson, M.D.; Weisbrod, R.M.; Pimental, D.R.; Tong, X.; Bolotina, V.M.; Cohen, R.A. Redox regulation of SERCA2 is required for vascular endothelial growth factor-induced signaling and endothelial cell migration. *Antioxid. Redox Signal.* **2012**, *17*, 1099–1108. [[CrossRef](#)] [[PubMed](#)]
74. Brailoiu, G.C.; Gurzu, B.; Gao, X.; Parkesh, R.; Aley, P.K.; Trifa, D.I.; Galione, A.; Dun, N.J.; Madesh, M.; Patel, S.; et al. Acidic NAADP-sensitive calcium stores in the endothelium: Agonist-specific recruitment and role in regulating blood pressure. *J. Biol. Chem.* **2010**, *285*, 37133–37137. [[CrossRef](#)] [[PubMed](#)]

75. Favia, A.; Desideri, M.; Gambarà, G.; D'Alessio, A.; Ruas, M.; Esposito, B.; Del Bufalo, D.; Parrington, J.; Ziparo, E.; Palombi, F.; et al. VEGF-induced neoangiogenesis is mediated by NAADP and two-pore channel-2-dependent  $\text{Ca}^{2+}$  signaling. *Proc. Natl. Acad. Sci. USA* **2014**, *111*, E4706–E4715. [[CrossRef](#)]
76. Gambarà, G.; Billington, R.A.; Debidà, M.; D'Alessio, A.; Palombi, F.; Ziparo, E.; Genazzani, A.A.; Filippini, A. NAADP-induced  $\text{Ca}^{2+}$  signaling in response to endothelin is via the receptor subtype B and requires the integrity of lipid rafts/caveolae. *J. Cell. Physiol.* **2008**, *216*, 396–404. [[CrossRef](#)]
77. Balbi, C.; Lodder, K.; Costa, A.; Moimas, S.; Moccia, F.; van Herwaarden, T.; Rosti, V.; Campagnoli, F.; Palmeri, A.; de Biasio, P.; et al. Reactivating endogenous mechanisms of cardiac regeneration via paracrine boosting using the human amniotic fluid stem cell secretome. *Int. J. Cardiol.* **2019**, *287*, 87–95. [[CrossRef](#)]
78. Martucci, L.L.; Cancela, J.M. Neurophysiological functions and pharmacological tools of acidic and non-acidic  $\text{Ca}^{2+}$  stores. *Cell Calcium* **2022**, *104*, 102582. [[CrossRef](#)]
79. Foster, W.J.; Taylor, H.B.C.; Padamsey, Z.; Jeans, A.F.; Galione, A.; Emptage, N.J. Hippocampal mGluR1-dependent long-term potentiation requires NAADP-mediated acidic store  $\text{Ca}^{2+}$  signaling. *Sci. Signal.* **2018**, *11*, eaat9093. [[CrossRef](#)]
80. Pereira, G.J.; Hirata, H.; Fimia, G.M.; do Carmo, L.G.; Bincoletto, C.; Han, S.W.; Stilhano, R.S.; Ureshino, R.P.; Bloor-Young, D.; Churchill, G.; et al. Nicotinic acid adenine dinucleotide phosphate (NAADP) regulates autophagy in cultured astrocytes. *J. Biol. Chem.* **2011**, *286*, 27875–27881. [[CrossRef](#)]
81. Galione, A. NAADP Receptors. *Cold Spring Harb. Perspect. Biol.* **2019**, *11*, a035071. [[CrossRef](#)] [[PubMed](#)]
82. Ronco, V.; Potenza, D.M.; Denti, F.; Vullo, S.; Gagliano, G.; Tognolina, M.; Guerra, G.; Pinton, P.; Genazzani, A.A.; Mapelli, L.; et al. A novel  $\text{Ca}^{2+}$ -mediated cross-talk between endoplasmic reticulum and acidic organelles: Implications for NAADP-dependent  $\text{Ca}^{2+}$  signalling. *Cell Calcium* **2015**, *57*, 89–100. [[CrossRef](#)] [[PubMed](#)]
83. Morgan, A.J.; Davis, L.C.; Wagner, S.K.; Lewis, A.M.; Parrington, J.; Churchill, G.C.; Galione, A. Bidirectional  $\text{Ca}^{2+}$  signaling occurs between the endoplasmic reticulum and acidic organelles. *J. Cell Biol.* **2013**, *200*, 789–805. [[CrossRef](#)] [[PubMed](#)]
84. Atakpa, P.; Thillaiappan, N.B.; Mataragka, S.; Prole, D.L.; Taylor, C.W. IP3 Receptors Preferentially Associate with ER-Lysosome Contact Sites and Selectively Deliver  $\text{Ca}^{2+}$  to Lysosomes. *Cell Rep.* **2018**, *25*, 3180–3193.e7. [[CrossRef](#)]
85. Pitt, S.J.; Reilly-O'Donnell, B.; Sitsapesan, R. Exploring the biophysical evidence that mammalian two-pore channels are NAADP-activated calcium-permeable channels. *J. Physiol.* **2016**, *594*, 4171–4179. [[CrossRef](#)]
86. Blatter, L.A. Tissue Specificity: SOCE: Implications for  $\text{Ca}^{2+}$  Handling in Endothelial Cells. *Adv. Exp. Med. Biol.* **2017**, *993*, 343–361. [[CrossRef](#)]
87. Avila-Medina, J.; Mayoral-Gonzalez, I.; Dominguez-Rodriguez, A.; Gallardo-Castillo, I.; Ribas, J.; Ordonez, A.; Rosado, J.A.; Smani, T. The Complex Role of Store Operated Calcium Entry Pathways and Related Proteins in the Function of Cardiac, Skeletal and Vascular Smooth Muscle Cells. *Front. Physiol.* **2018**, *9*, 257. [[CrossRef](#)]
88. Moccia, F.; Dragoni, S.; Poletto, V.; Rosti, V.; Tanzi, F.; Ganini, C.; Porta, C. Orai1 and Transient Receptor Potential Channels as novel molecular targets to impair tumor neovascularisation in renal cell carcinoma and other malignancies. *Anticancer. Agents Med. Chem.* **2014**, *14*, 296–312. [[CrossRef](#)]
89. Schleifer, H.; Doleschal, B.; Lichtenegger, M.; Oppenrieder, R.; Derler, I.; Frischauf, I.; Glasnov, T.N.; Kappe, C.O.; Romanin, C.; Groschner, K. Novel pyrazole compounds for pharmacological discrimination between receptor-operated and store-operated  $\text{Ca}^{2+}$  entry pathways. *Br. J. Pharmacol.* **2012**, *167*, 1712–1722. [[CrossRef](#)]
90. Zuccolo, E.; Lim, D.; Kheder, D.A.; Perna, A.; Catarsi, P.; Botta, L.; Rosti, V.; Riboni, L.; Sancini, G.; Tanzi, F.; et al. Acetylcholine induces intracellular  $\text{Ca}^{2+}$  oscillations and nitric oxide release in mouse brain endothelial cells. *Cell Calcium* **2017**, *66*, 33–47. [[CrossRef](#)]
91. Montes de Oca Balderas, P. Flux-Independent NMDAR Signaling: Molecular Mediators, Cellular Functions, and Complexities. *Int. J. Mol. Sci.* **2018**, *19*, 3800. [[CrossRef](#)] [[PubMed](#)]
92. Dore, K.; Stein, I.S.; Brock, J.A.; Castillo, P.E.; Zito, K.; Sjöstrom, P.J. Unconventional NMDA Receptor Signaling. *J. Neurosci.* **2017**, *37*, 10800–10807. [[CrossRef](#)] [[PubMed](#)]
93. Balasubramanian, S.; Teissere, J.A.; Raju, D.V.; Hall, R.A. Hetero-oligomerization between GABAA and GABAB receptors regulates GABAB receptor trafficking. *J. Biol. Chem.* **2004**, *279*, 18840–18850. [[CrossRef](#)] [[PubMed](#)]
94. Shrivastava, A.N.; Triller, A.; Sieghart, W. GABA(A) Receptors: Post-Synaptic Co-Localization and Cross-Talk with Other Receptors. *Front. Cell. Neurosci.* **2011**, *5*, 7. [[CrossRef](#)]